© 2018 IJSRSET | Volume 4 | Issue 4 | Print ISSN: 2395-1990 | Online ISSN : 2394-4099
Themed Section : Engineering and Technology

Classification Detection of Ftir And Xrd Spectrum on Thin Film of Lithium Tantalate With Arima Model On High Level Accuracy

Muhammad Nur Aidi[1] and Irzaman[2]

[1]Department of Statistics, Faculty of Mathematics and Sciences Natural (FMIPA), Bogor Agricultural University (IPB), Kampus IPB Dramaga Bogor Indonesia

[2]Department of Physics, Faculty of Mathematics and Sciences Natural (FMIPA), Bogor Agricultural University (IPB), Kampus IPB Dramaga Bogor Indonesia

ABSTRACT

Lithium tantalate ($LiTaO_3$) is very good for electrooptical modulator and pyroelectric detector. Therefore, $LiTaO_3$ detection was very important to get the deeper image of its material characteristics. $LiTaO_3$ detection methods were such as X-ray powder diffraction (XRD), and Fourier-transform infrared spectroscopy (FTIR and were then modelled by Reietveld model or General Structure Analysis System (GSAS) which were based on reference pattern as comparison. ARIMA model could also be used as alternative. ARIMA model did not need reference pattern as comparison. ARIMA models classify XRD and FTIR data to autoregression non differencing models. ARIMA model for Lanthanum Oxide (0%, 5 %, 10 %) doped Lithium Tantalate FTIR were ARIMA (3,0,1), ARIMA (3,0,0), ARIMA (3,0,1) which are R^2 value of ARIMA model which exceed 80% (94%, 94%, 97%). ARIMA model for Lanthanum Oxide (0%, 5 %, 10 %) doped Lithium Tantalate XRD were ARIMA (5,0,1), ARIMA (5,0,1), ARIMA (7,0,0) which are R^2 value of 91%, 92%, 87%.ARIMA model for FTIR value was simpler and has lower MAPE than ARIMA model for XRD value. Lithium Tantalate doping with 5% and 10% Lanthanum Oxide could decrease the FTIR and XRD value control.

Keywords: Lithium Tantalate, Lanthanum Oxide, XRD, FTIR, ARIMA, Determinancy coeficiency (R^2), MAPE

I. INTRODUCTION

E Lithium tantalate ($LiTaO_3$) was very potential to be developed as light, temperature, and pressure sensor (Trybula et al. 2016; Damodaran et al 2016). This material was very promising for science and technology of new device development Hiranaga et al. 2009; Jesse et al. 2012; Bartasyte et al. 2017), due to its unique characteristics such as its sensitivity towards light, temperature and pressure (Kang et al. 2007; Gorelik et al. 2017). Lithium tantalate (LiTaO3) was a ferroelectric material (Sun et al. 2014; Izyumskaya et al. 2013) which had unique characteristic of pyroelectric and piezoelectric which combined with good mechanical and chemical stability. As ferroelectric material, Lithium tantalate ($LiTaO_3$) expected to apply its pyroelectric characteristic as infrared sensor. Thus, $LiTaO_3$ was usually used for several application such as electro-optical modulator and pyroelectric detector (Shur et al. 2017). LiTaO3 was non-hygroscopic crystal, non colored, water soluble, high transmission level, and optical characterisitc that did not easy to be damaged. LiTaO3 was material which had high dielectric constant and high voltage capacity (Liang et al. 2015).

Ferroelectric material had been extensively studied as thin film (Kalinin et al 2016; Sidorkin et al. 2014; Yanga et al. 2014; Chang et al. 2017), especially applied as multilayer ceramic capacitor (MLCC) (Khan et al. 2015) and Dynamic Random Access Memory (DRAM) (Sharma et al. 2015). Among many type of ferroelectric material, Lithium tantalate (LiTaO3) was the most extensively studied becaused of its high dielectric constant (Li et al. 2014; Yoo et al. 2012), low dielectric loss, and good thermal stability (Vogela et al. 2016; Edwards 2017).

LiTaO3 powder and thin film usually made by solid-state reaction (Li et al. 2014), sol-gel (Yanga et al. 2014; Aguas et al. 2001), and hidrothermal method (Vogela et al. 2016). Various innovative approach, such as spray pyrolisis, oxidation synthetizing, co-chemical precipitation, pulsed laser deposition (PLD), chemical vapor deposition (CVD), electrochemical, spray electrostatic vapor deposition, had been used to synthesize $LiTaO_3$ powder (Garten et al. 2016). $LiTaO_3$ characteristic was very dependent on its composition, mineral structure, and its molecular geometry. Therefore, LiTaO3 detection was very important to get the deeper image of its material characteristics (Garten et al. 2016; Lines 1972).

LiTaO3 detection methods were such as X-ray powder diffraction (XRD), and Fourier-transform infrared spectroscopy (FTIR) (Tavakoli et al 2013). X-ray powder diffraction (XRD) was a fast analysizing method which especially used for identifying crystal material fase and could give information about unit cell dimension. Analyzed material should be composition of smooth, homogenesis, and composition (Althowibi 2017; Morozova 2010). X-ray diffraction (Althowibi 2017) based on monochromatic X-ray constructive interference (Morozova 2010) and crystal sample.

X-ray produced by cathode ray tube (Barbieri 2005) was filtered to creat monochromatic radiation (Donativi et al. 2007), collimated to consentrated and point to the sample. Occuring ray interraction with the sample created constructive interference (Coleman et al. 2015) (and ray diffracted) if the condition met the Bragg Law ($n\lambda = 2d \sin \theta$) (Soshnikov et al. 2017). This law connected the electromagnetic radiation wavelength with the diffraction angle and grid length in the crystal sample. The diffracted X-ray was then detected, proceed, and calculated. By scanning the sample through 2θ angles range, all possible direction grid diffraction should be achieved because of the random orientation of powder material. Diffraction peak conversion (Asadchikov et al. 2009) to d-distance made it possible to identify mineral because each mineral has unique d-distance. Usually, it was done by ration d-distance with the standard reference pattern (Sharma 2015).

Fourier-transform Infrared spectroscopy [FTIR] was a method used to retrieve gas-solid, solid or gas absorbtion or emission infrared spectrum. A FTIR spectrometer simultanously collected high spetrum resolution data through wide spectrum range (Chowdhurya 2017; Dzunuzovic 2015). This gives significant advantage over dispersive spectrometer which measures intensity in narrow wave range in one set of time. Fourier-transform Infrared spectroscopy term was derived from the fact that Fourier transformation (mathematical process) was needed to convert the raw data to the actual spectrum (Chowdhurya 2017; Dzunuzovic 2015; Justin et al. 2017; Bijay et al. 2017; Nagahi et al. 2017).

From the explanation above, studying atomic and molecular structure $LiTaO_3$ is very important in terms of studying the optical, electrical, mechanical and crystal characteristic of thin film or solid state LiTaO3 (Irzaman et al. 2016; Juraschek et al. 2017; Anokhina et al. 2016). Atomic and molecular structure could be studied through reflectant function which derived from XRD spectrum (Varga et al. 2017; Benzaouak et al. 2017; Reddy et al. 2017; Du et al. 2015; Ding et al. 2017) and FTIR spectrum (Naghi et al. 2017; Ianculescu et al. 2015) value through ARIMA model approach (Liu et al. 2017; Aidi et al. 2013; Nochai 2006; Hana et al. 2010; Widowatia et al. 2016; Nelson 1998; Khandelwa et al. 2015; De´gerine et al. 2003; Medeiros 2008; Elmaleh 2017; Mohan et al. 2017; Oliveira et al. 2017; Koutroumanidis et al. 2009; Qin et al. 2017).

II. Research Objectives

1. To retrieve ARIMA function for $LiTaO_3$ thin film from FTIR and XRD data spectrum
2. To compare ARIMA function for $LiTaO_3$ thin film from FTIR and XRD data spectrum which doped with Lanthanum Oxide (0 %, 5 % dan 10 %)

III. Research Methodology

The thin films preparation was started by cutting the Si substrate with the size of 8 mm × 8 mm. Then, the substrates were cleaned using aqua bidest and dried. In this case, three $LiTaO_3$ solutions were prepared using CSD (Chemical Solution Deposition) method. The first solution was prepared by mixing 0.1650 gram of $LiCH_3COO$ and 0.5524 gram of Ta_2O_5 which were soluted inside 2.5 ml of 2-metoxy methanol which called undoped $LiTaO_3$ solution. The second solution was prepared bymixing 0.1650 gram of $LiCH_3COO$ and 0.5524 gram of Ta_2O_5 which were soluted $LiTaO_3$2.5 ml of 2-metoxy methanol with the addition of 0.0295 gram of La_2O_5 as dopant which called 5% lanthanum doped $LiTaO_3$ solution. Afterwards, the third solution was prepared by mixing 0.1650 gram of $LiCH_3COO$ and 0.5524 gram of Ta_2O_5 which were soluted inside 2.5 ml of 2-metoxy methanol with the addition of 0.0590 gram of La_2O_5 which called 10% lanthanum doped $LiTaO_3$ solution.After the preparation of those three solutions, they were sonificated for 90 minutes using Branson 2510. Afterwards, the solution was dropped towards the substrate's surfaceon spin coating rotator with speed of 3000 rpm, conducted twice. The remaining solutionthen dried at 80◦C for 24 hours. The droppedsubstrate was then annealed using Furnace with the increasing rate of temperature at1.7◦C/minute, started from room temperature until it reaches 550◦C and held constantlyfor 12.5 hours, and then cooled down into room temperature.Then characterized using FTIR and XRD (Irzaman et al. 2015).

FTIR spectrum characterization from $LiTaO_3$ thin film used FTIR tools type ABB MB 3000. In this research, FTIR spectrum used belongs to the mid infared radiaton category (wavenumber of 4000-500 cm^{-1}) with step of 16 cm^{-1}. XRD spectrum characterization used the XRD tools type GBC EMMA. In this research XRD spectrum used belongs to angle range of 10^0 to 80^0 with step of 0.02^0 (Irzaman et al. 2003; 2013; 2015; 2016; Yogaraksa et al. 2004; Darmasetiawan 2002).

ARIMA model exploration for FTIR and XRD value was done by Box and Jenkin procedure (George et al. 1970). Initial step was done to classify the data was stationary or not in mean and in variance. Augmented Dickey-Fuller will be used. A**augmented Dickey–Fuller test** (**ADF**) tests the null hypothesis that a unit root is present in a time series sample. The alternative hypothesis is different depending on which version of the test is used, but is usually stationarity or trend-stationarity. It is an augmented version of the Dickey–Fuller test for a larger and more complicated set of time series models (Dickey et al. 1979). If it was not stationary in mean then differencing need to be done, and transformation needs to be done if it was not stationary in variance. If the data was stationary, then ACF (Autocorrelation Function) plot and PACF (Partial Autocorrelation Function) plot were done to get possible assumption model, which classify data to autoregression (AR) and moving average (MA) or both models (George et al. 1970). Next step was to get estimated parameter model and to test the parameter to the models until significant model parameters were obtained. Selected model was then calculated its determinancy coeficient value (R^2), Mean Absolut Percentage Error (MAPE), and plotted with the XRD dan FTIR actual and predicted data to determine the accuracy of the model (Aidi et al. 2013). In this research, we used SAS 9.4 32 bit academic version and Lenovo Computer 2 GB 64 Bit.

IV. Result and Discussion

4.1. Raw Data

Plot between infrared wavelength value as x-axis and absorbed, reflected, and transmitted percent of infrared as the y-axis on control Lanthanum Oxide (0%) doped Lithium Tantalate was showed in Figure 1. Meanwhile in Figure 2 and Figure 3, it showed Plot between infrared wavelength value and absorbed, reflected, and transmitted percent of infrared Lanthanum Oxide (5%, 10%, respectively) doped Lithium Tantalate.

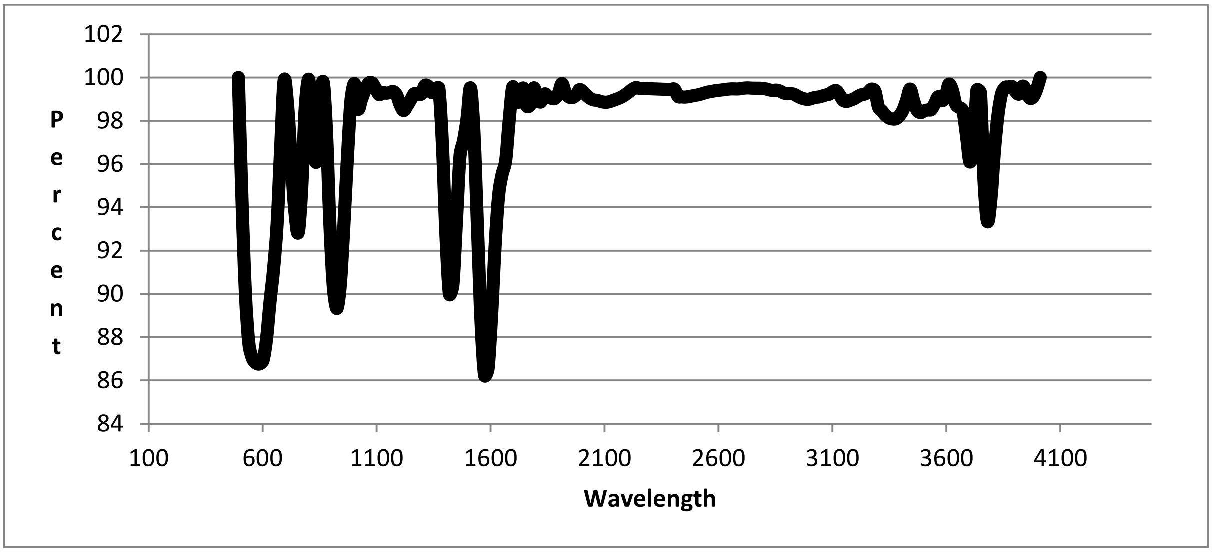

Figure 1. Plot between infrared wavelength value and absorbed, reflected, and transmitted percent of infrared on control Lanthanum Oxide (0%) doped Lithium Tantalate

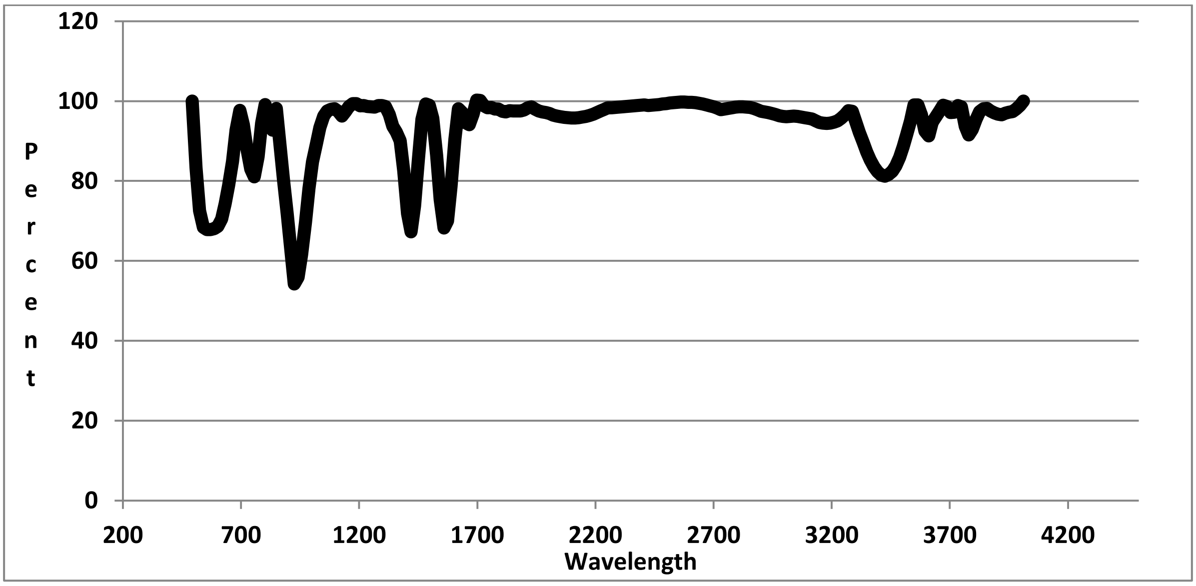

Figure 2. Plot between infrared wavelength value and absorbed, reflected, and transmitted percent of infrared on Lanthanum Oxide (5%) doped Lithium Tantalate

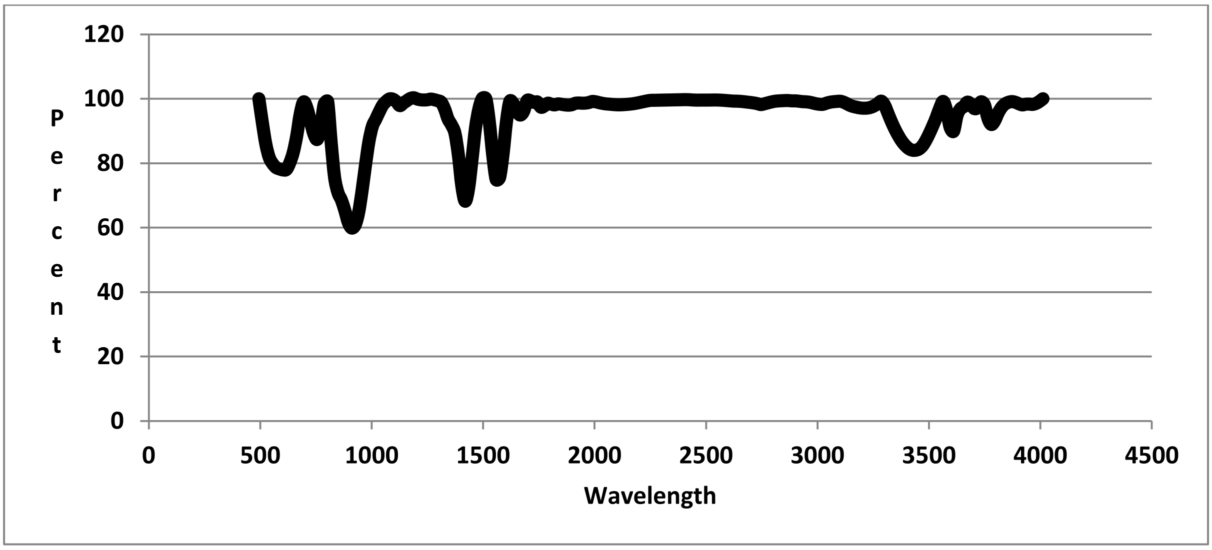

Figure 3. Plot between infrared wavelength value and absorbed, reflected, and transmitted percent of infrared on Lanthanum Oxide (10%) doped Lithium Tantalate

To model the spectrum data on Figure 1, 2, 3, there was assumption that observation value (percentage of absorbed, reflected, and transmitted) of t-wavelength was function of wavelength observation value t-1, t-2, t-k. Thus, x-axis value could be substitued with integer number 1, 2, 3,.. which were consistent with wavelength value 1, 2, 3,.... Thus, Figure 1, 2, and 3 could be substitued with Figure 4, 5, and 6 (Aidi et al. 2013; 2017).

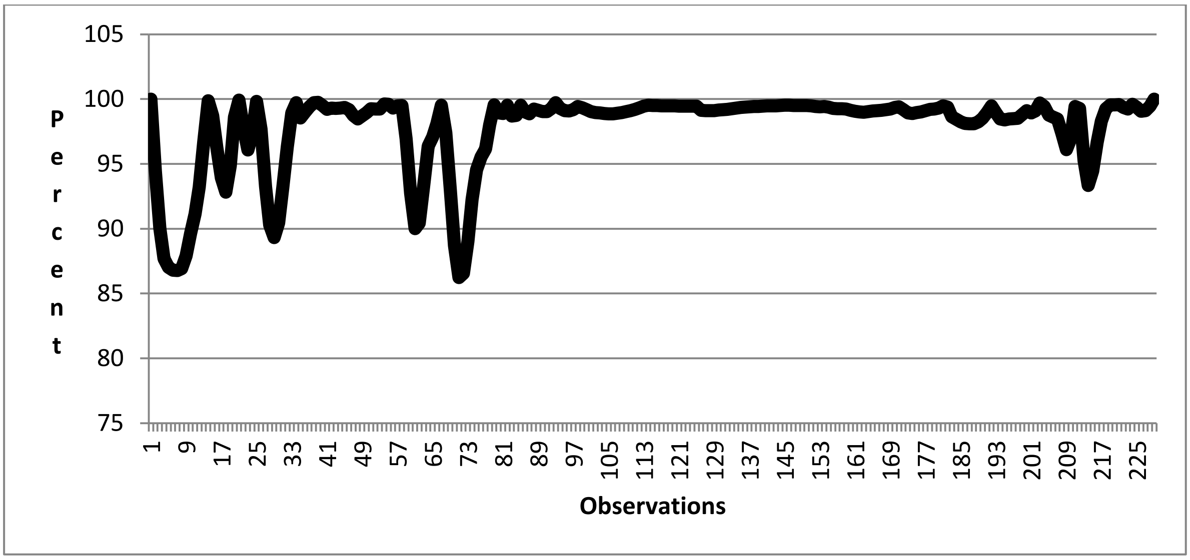

Figure 4. Plot between observation order and absorbed, reflected, and transmitted percentage (FTIR) on Lanthanum Oxide (0%) doped Lithium Tantalate

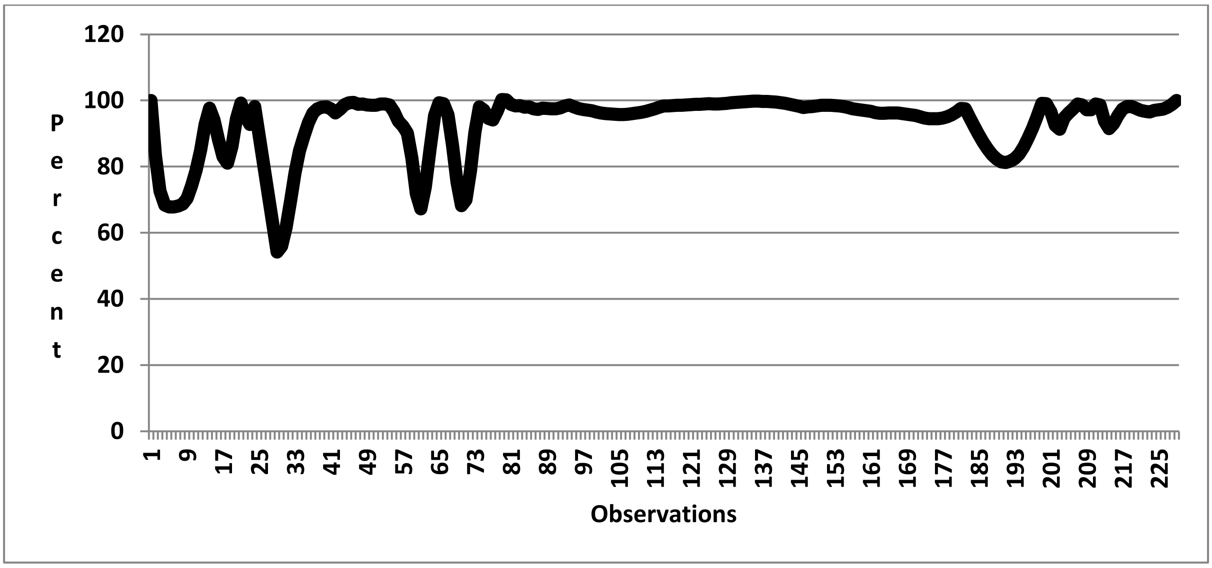

Figure 5. Plot between observation order and absorbed, reflected, and transmitted percentage (FTIR) on Lanthanum Oxide (5%) doped Lithium Tantalate

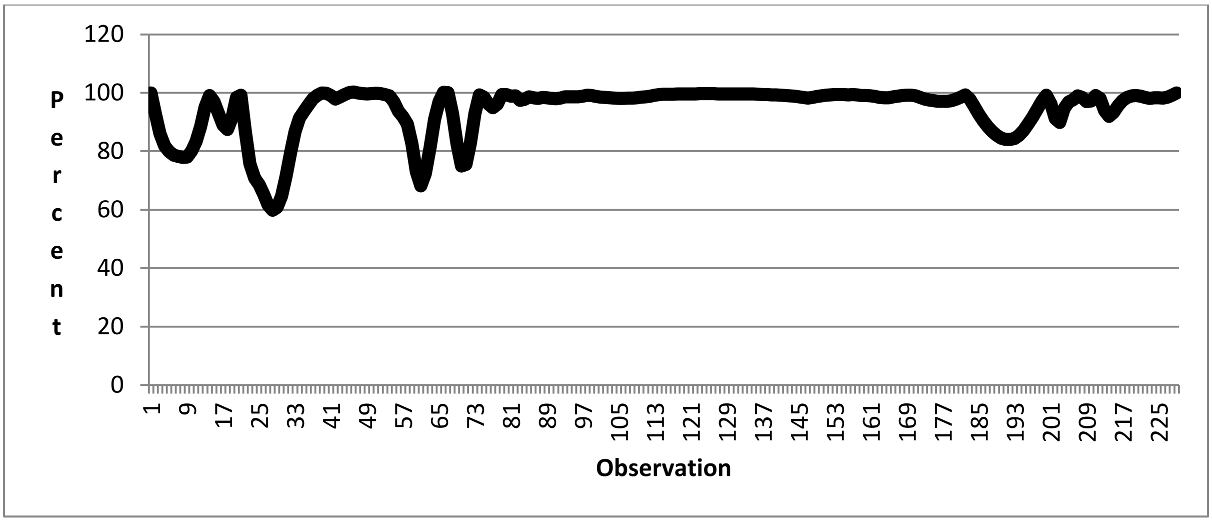

Figure 6. Plot between observation order and absorbed, reflected, and transmitted percentage (FTIR) on Lanthanum Oxide (10%) doped Lithium Tantalate

Figure 7, 8, 9 were plot between X-ray angle as x-axis and reflected intensity value as y-axis on Lanthanum Oxide (0%, 5%, 10%) doped Lithium Tantalate

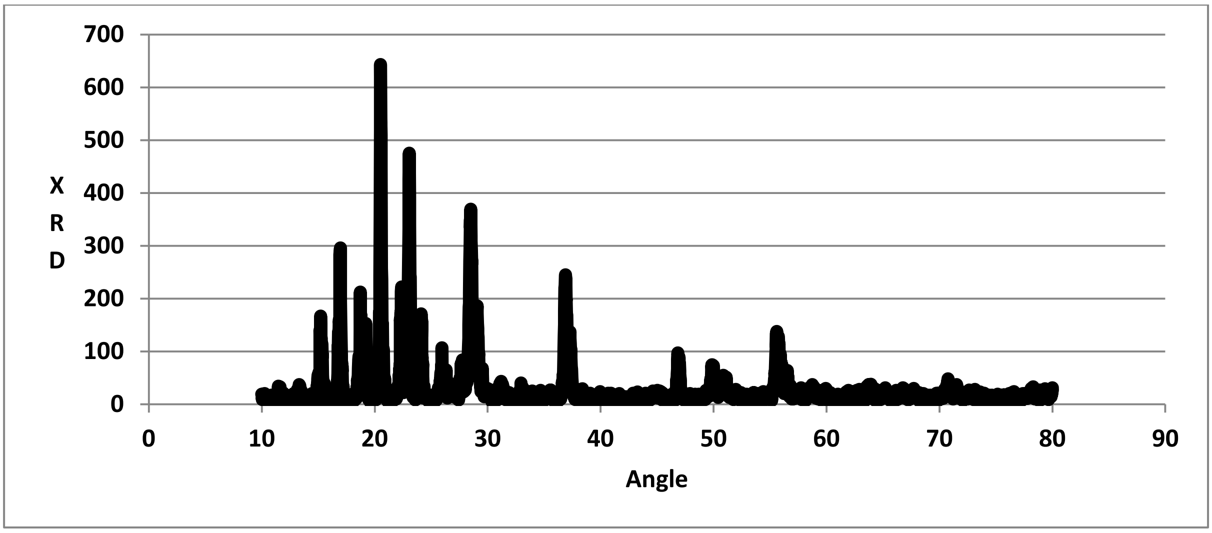

Figure 7. Plot between X-ray angle and XRD Intensity on Lanthanum Oxide (0%) doped Lithium Tantalate

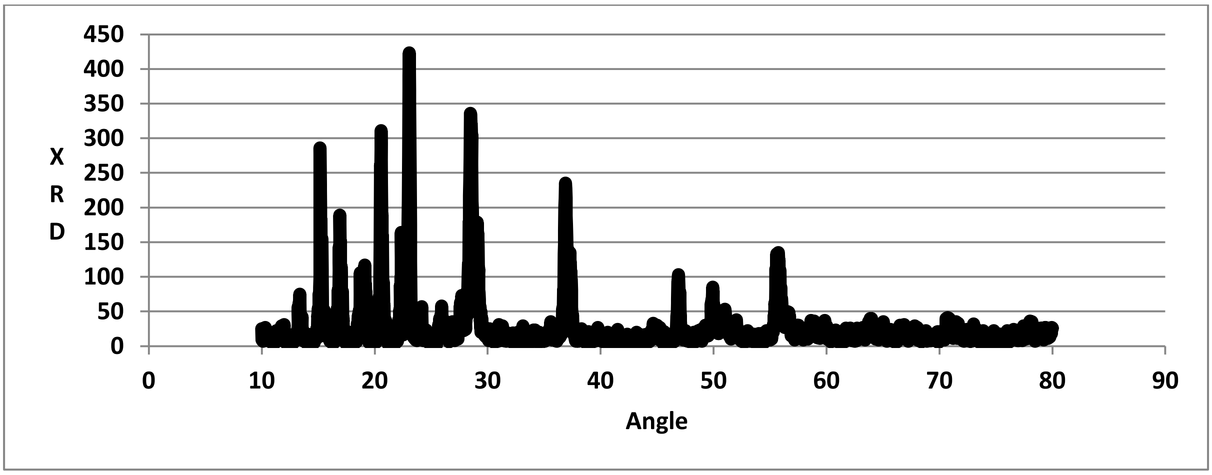

Figure 8. Plot between X-ray angle and XRD Intensity on Lanthanum Oxide (5%) doped Lithium Tantalate

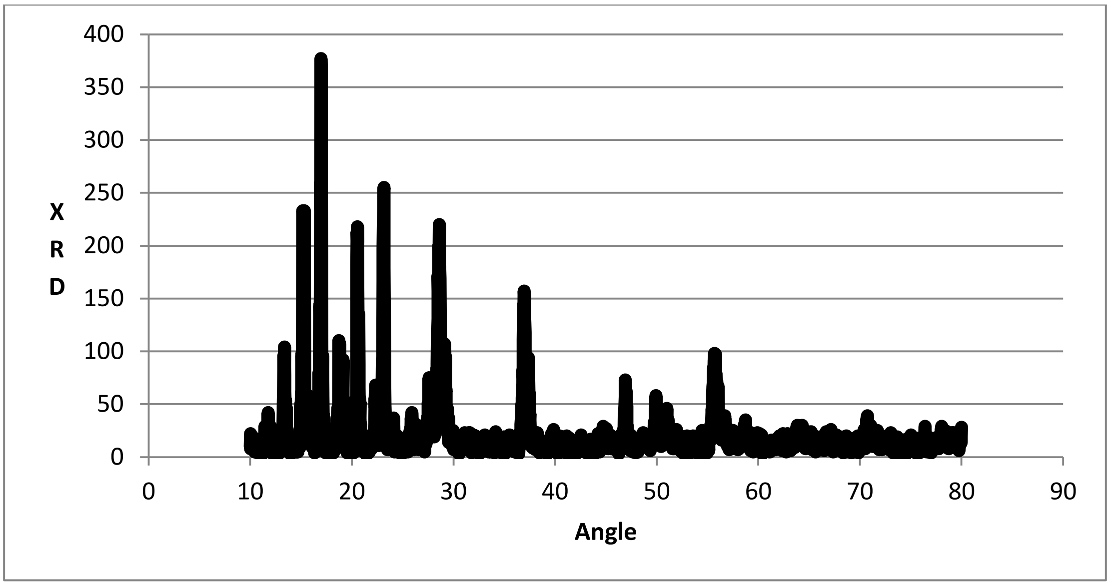

Figure 9. Plot between X-ray angle and XRD intensity on Lanthanum Oxide (10%) doped Lithium Tantalate

Then, x-axis value on Figure 7, 8, 9 were substitued into series number 1, 2, and so on which showed in Figure 10, 11, 12 (Aidi et al. 2013; 2017).

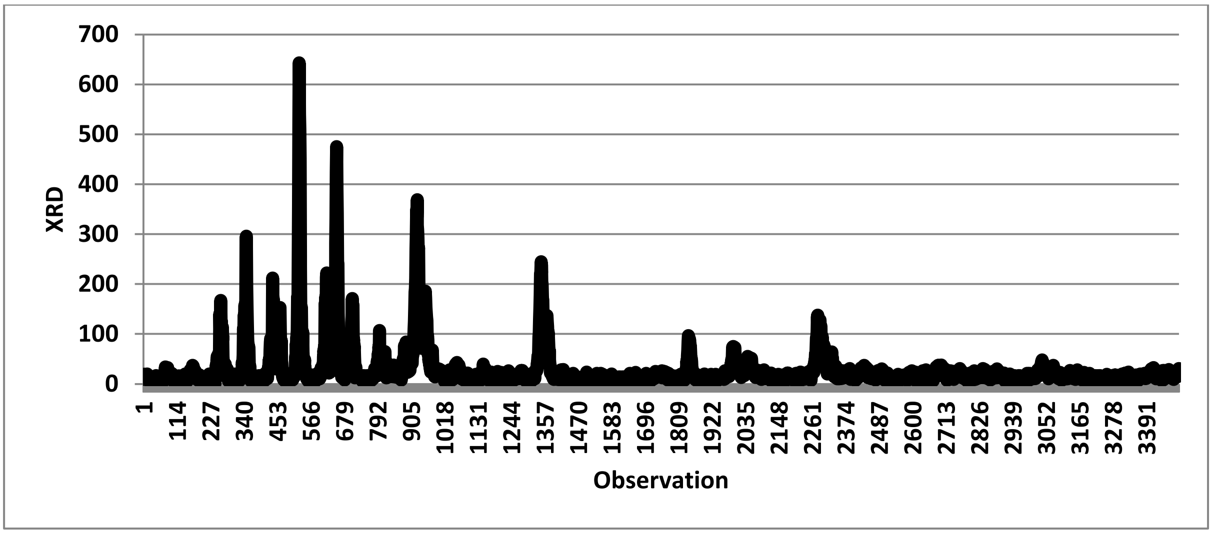

Figure 10. Plot between observation order and XRD Intensity on Lanthanum Oxide (0%) doped Lithium Tantalate

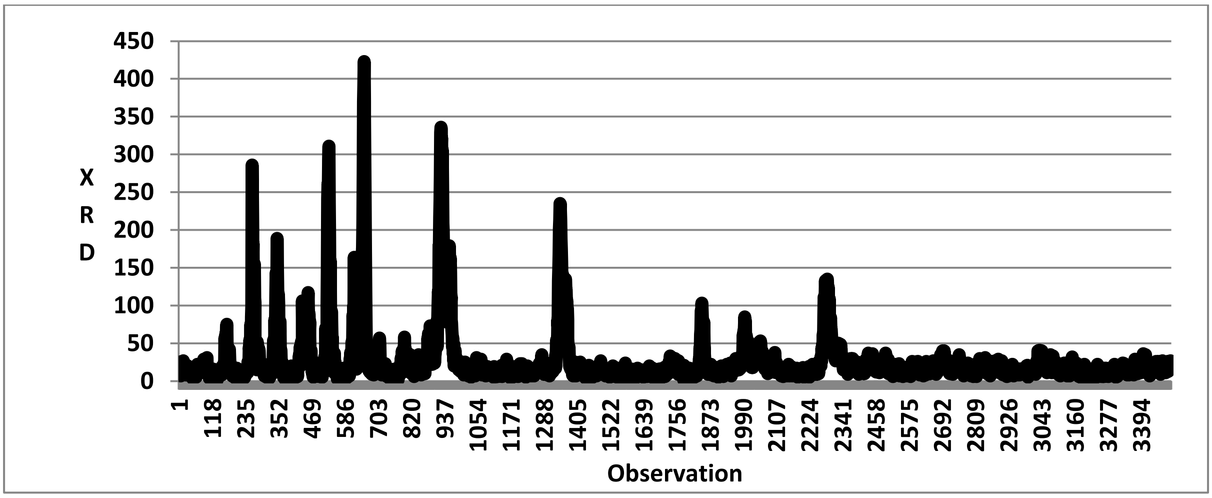

Figure 11. Plot between observation order and XRD Intensity Lanthanum Oxide (5%) doped Lithium Tantalate

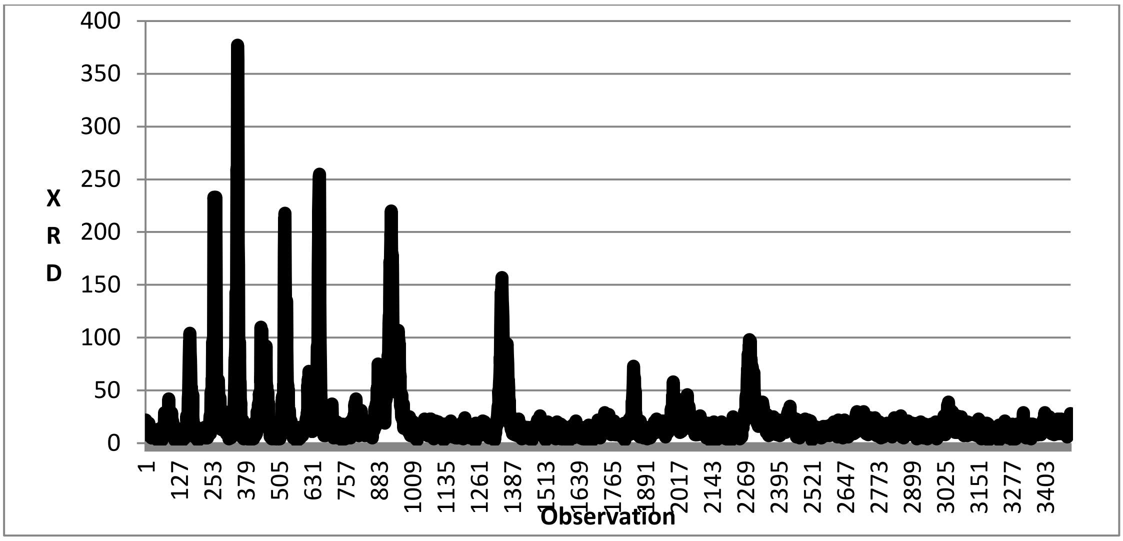

Figure 12. Plot between observation order and XRD Intensity Lanthanum Oxide (10%) doped Lithium Tantalate

4.2. ARIMA on Lithium Tantalate thin film FTIR spectrum

Lanthanum Oxide (0%) doped Lithium Tantalate data on Figure 4, Lanthanum Oxide (5%) doped Lithium Tantalate data on Figure 5, and Lanthanum Oxide (10 %) doped Lithium Tantalate data on Figure 6 were examined on stationary average with Augmented Dickey-Fuller. All test result showed with p-value < 0.0001 on stationary average. Thus, developed ARIMA models were non-differensing models for Lanthanum Oxide (0%, 5 %, 10 %) doped Lithium Tantalate data.

4.2.1. FTIR Spectrum on thin film of Lanthanum Oxide (0%) doped Lithium Tantalate

Plotting ACF and PACF which showed in Figure 13. Based on ACF and PACF plot, the possible tentative models were ARIMA (3,0,0), ARIMA(2,0,0), ARIMA(1,0,0). To select the best 3 ARIMA models, AIC (Akaike Information Criteria) calculation was done by choosing the smallest AIC. The result was showed Table 1. Model with minimum AIC value was the best model. Based on Table 1, ARIMA model (3,0,0) was the best.

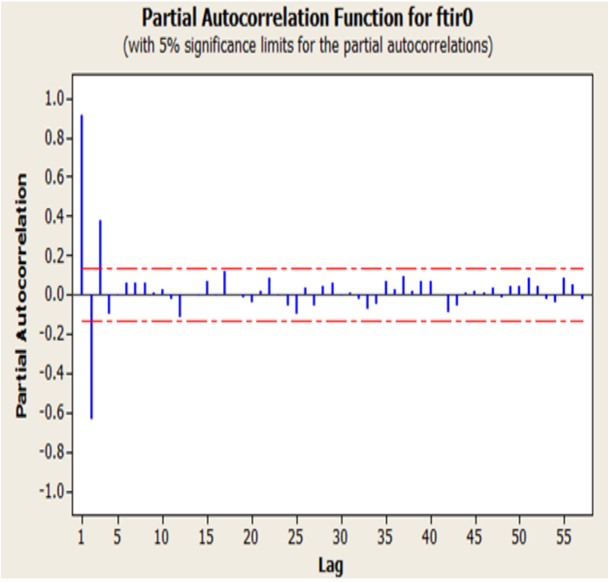

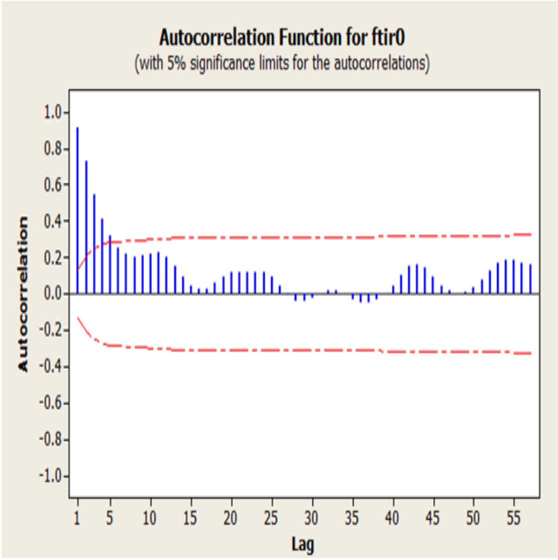

Figure 13. Plot of ACF and PACF on Lanthanum Oxide (0%) Doped Lithium Tantalate FTIR data.

Table 1. AIC value for ARIMA (3,00), ARIMA (2,00) and ARIMA (1,00) Lanthanum Oxide (0%) Doped Lithium Tantalate FTIR data

Model	AIC
ARIMA (3,0,0)	545.4589
ARIMA (2,0,0)	633.5049
ARIMA (1,0,0)	760.8167

Prediction result of ARIMA (3,0,0) of model coefficient showed that all predicted coefficients showed significanct. Model parameters predicted value were showed in Table 2.

Table 2. ARIMA (3,0,0) Model Coefficient Predicted Value of Lanthanum Oxide (0%) Doped Lithium Tantalate FTIR data

Parameter	Estimate	Standard Error	T Value	Approx Pr>|t|	lag
MU	102.53497	0.51077	200.75	<0.0001	0
AR1,1	2.00540	0.05389	37.21	<0.0001	1
AR1,2	-1.61261	0.09606	-16.79	<0.0001	2
AR1,3	0.58964	0.05393	10.93	<0.0001	3

Based on the ARIMA (3,0,0) model that was pointed above, order combination addition was done on ARIMA (3,0,0) model to get several ARIMA models those were predicted to get the best model (Table 3).

Table 3. ARIMA (3,0,0) Model Overfitting on Lanthanum Oxide (0%) Doped Lithium Tantalate FTIR Data

Model	AIC
ARIMA(3,0,0)	545.4589
ARIMA(4,0,0)	525.1741
ARIMA(3,0,1)	510.8595
ARIMA(4,0,1)	512.7956

Based on the table above, ARIMA (3,0,1) model was the best model. Therefore, ARIMA (3,0,0) was fixed by repredict with ARIMA (3,0,1) model. The reprediction result, ARIMA (3,0,1) model, was showed in Table 4. Based on Table 4, all parameters were significant.

Table 4. ARIMA (3,0,1) Model Coefficient Prediction Value on Lanthanum Oxide (0%) Doped Lithium Tantalate FTIR Data

Parameter	Estimate	Standard Error	T Value	Approx Pr>|t|	lag
MU	102.74934	0.33232	309.18	<0.0001	0
MA1,1	-0.61169	0.07096	-8.62	<0.0001	1
AR1,1	1.67220	0.08052	22.77	<0.0001	1
AR1,2	-1.07331	0.14073	-7.63	<0.0001	2
AR1,3	0.37093	0.076-9	4.87	<0.0001	3

Assumption on ARIMA model was independent residuals and normal distribution. Therefore, ARIMA (3,0,1) model residual was undergone test on independence (Table 5) and normality (Figure 14). The test result showed that ARIMA (3,0,1) model residual was independent and normally distributed (Table and graph below).

Table 5. Test on Independence of Error of ARIMA (3,0,1) on Lanthanum Oxide (0%) Doped Lithium Tantalate FTIR Data

To Lag	Chi-Square	DF	Pr>ChiSq	Autocorrelation					
6	1.27	2	0.5310	0.004	-0.014	-0.014	0.004	-0.064	-0.029
12	19.18	8	0.0139	-0.111	-0.043	0.090	-0.129	0.188	-0.006
18	22.32	14	0.0722	0.049	-0.046	0.023	-0.058	-0.061	0.023
24	36.58	20	0.0131	-0.054	0.150	-0.015	0.066	-0.070	0.145
30	39.48	26	0.438	0.043	0.054	-0.038	-0.031	-0.061	0.017
36	45.54	32	0.0570	0.022	-0.044	0.132	0.009	-0.023	-0.045
42	53.57	38	0.0482	-0.033	-0.007	0.017	-0.032	-0.013	0.161

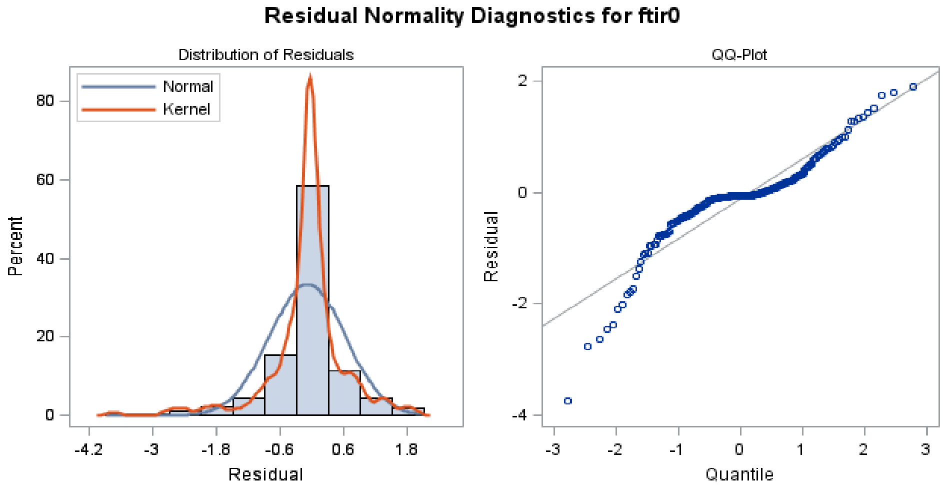

Figure 14. Test on Normality of Error of ARIMA (3,0,1) on Lanthanum Oxide (0%) Doped Lithium Tantalate FTIR Data

To make sure whether the ARIMA (3,0,1) good enough to predict FTIR pattern on Lanthanum Oxide (0%) doped Lithium Tantalate, plotting between predicted and actual data, and also Mean Absolut Percentage Error (MAPE) and R^2 calculation. The result showed that prediction plot of ARIMA (3,0,1) model (Figure 15) had approximated the its actual data, so the model was good enough to be a prediction. Resulted MAPE from the prediction was 0.45% and the R^2 was 94%.

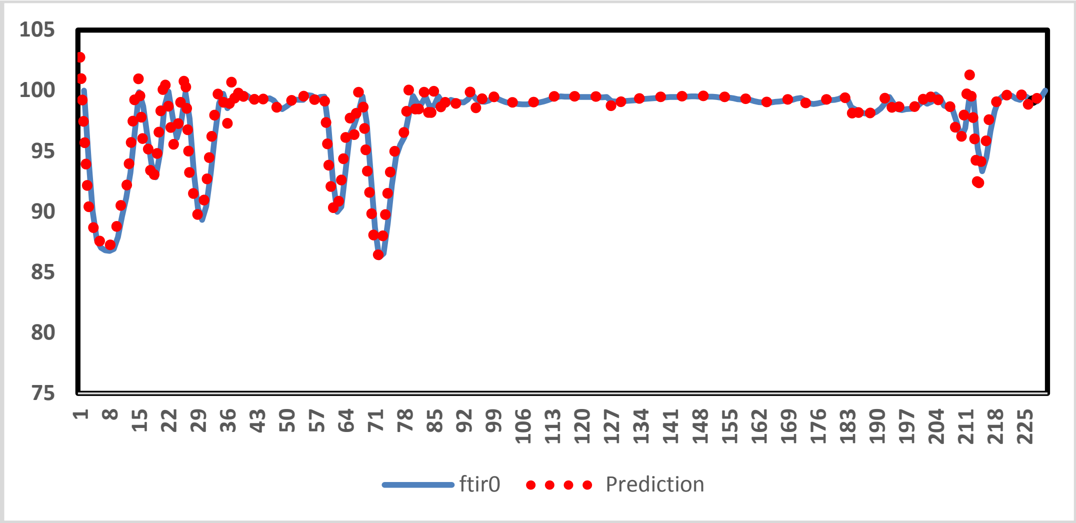

Figure 15. Plot of Actual Data and the Predicted Data of ARIMA (3,0,1) on FITR pattern of Lanthanum Oxide (0%) Doped Lithium Tantalate

From the process above, it could be concluded that FTIR pattern on Lanthanum Oxide (0%) Doped Lithium Tantalate could be well predicted by ARIMA (3,0,1) with the equation model (1):

$$y_t = 102.74934 + 1.67220\, y_{t-1} - 1.07331\, y_{t-2} + 0.37093\, y_{t-3} - 0.61169\, e_{t-1}. \quad (1)$$

4.2.2. FTIR Spectrum on thin film of Lanthanum Oxide (5%) doped Lithium Tantalate

Plotting of ACF and PACF which showed in Figure 16. Based on ACF and PACF plot, the possible tentative models were ARIMA (3,0,0), ARIMA(2,0,0), ARIMA(1,0,0). To select the best 3 ARIMA models, AIC (Akaike Information Criteria) calculation was done by choosing the smallest AIC. The result was showed Table 6. Model with minimum AIC value was the best model. Based on Table 6, ARIMA model (3,0,0) was the best.

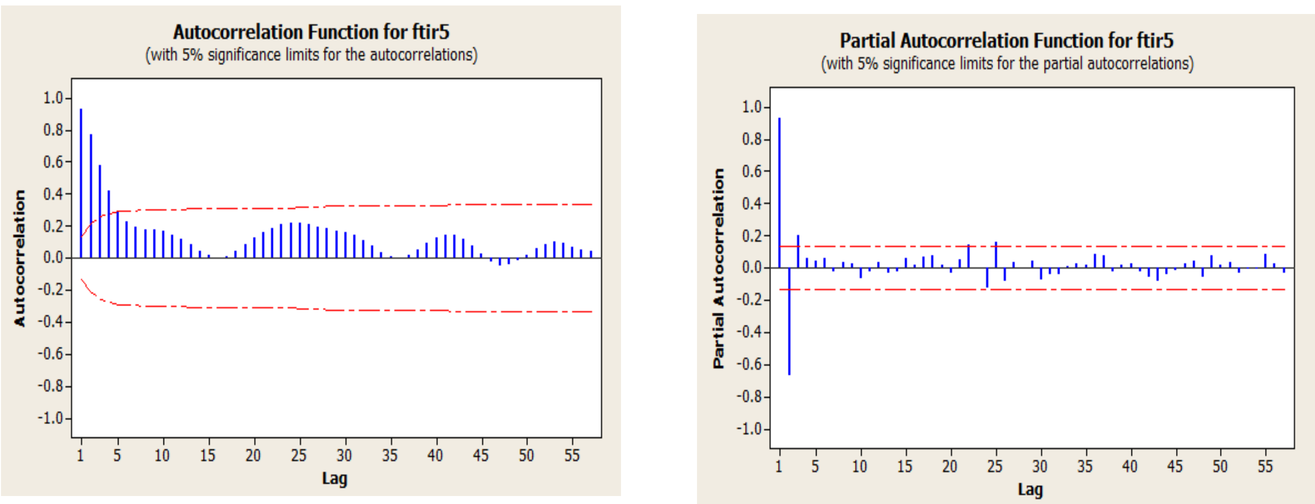

Figure 16. Plot of ACF and PACF on Lanthanum Oxide (5%) Doped Lithium Tantalate FTIR data.

Table 6. AIC value for ARIMA (3,0,0), ARIMA (2,0,0) and ARIMA (1,0,0) Lanthanum Oxide (5%) Doped Lithium Tantalate FTIR Data

Model	AIC
ARIMA (3,0,0)	992.0589
ARIMA (2,0,0)	1057.025
ARIMA (1,0,0)	1216.658

Prediction result of ARIMA (3,0,0) of model coefficient showed that all predicted coefficients showed significant. Model parameters predicted value were showed in Table 7. Based on Table 7, all parameters were significant.

Table 7. ARIMA (3,0,0) Model Coefficient Predicted Value of Lanthanum Oxide (5%) Doped Lithium Tantalate FTIR data

Parameter	Estimate	Standard Error	tValue	ApproxPr>|t|	lag
MU	108.60558	1.34918	80.50	<0.0001	0
AR1,1	2.06089	0.05722	36.02	<0.0001	1
AR1,2	-1.59078	0.10461	-15.21	<0.0001	2
AR1,3	0.51439	0.05732	8.97	<0.0001	3

Based on the ARIMA (3,0,0) model that was pointed above, order combination addition was done on ARIMA (3,0,0) model to get several ARIMA models those were predicted to get the best model (Table 8). Based on Table 8, ARIMA (3,0,0) model was the best model (lowest AIC). All ARIMA (3,0,0) model coeficients calculation result were significant (Table 9).

Tabel 8. ARIMA (3,0,0) Model Overfitting on Lanthanum Oxide (5%) Doped Lithium Tantalate FTIR Data

Model	AIC
ARIMA(3,0,0)	992.059
ARIMA(4,0,0)	993.340
ARIMA(3,0,1)	992.757
ARIMA(4,0,1)	996.044

Tabel 9. ARIMA (3,0,0) Model Coefficient Prediction Value on Lanthanum Oxide (5%) Doped Lithium Tantalate FTIR Data

Parameter	Estimate	Standard Error	tValue	ApproxPr>|t|	lag
MU	108.60558	1.34918	80.50	<0.0001	0
AR1,1	2.06089	0.05722	36.02	<0.0001	1
AR1,2	-1.59078	0.10461	-15.21	<0.0001	2
AR1,3	0.51439	0.05732	8.97	<0.0001	3

Assumption on ARIMA model was independent residuals and normal distribution. Therefore, ARIMA (3,0,0) model residual was undergone test on independence (Table 10) and normality (Figure 17). The test result showed that ARIMA (3,0,0) model residual was independent and normally distributed (Table and graph below).

Table 10. Test on Independence of Error of ARIMA (3,0,0) on Lanthanum Oxide (5%) Doped Lithium Tantalate FTIR Data

To Lag	Chi-Square	DF	Pr>ChiSq	Autocorrelation					
6	8.44	3	0.0377	0.029	-0.099	0.044	0.066	-0.137	-0.010
12	17.28	9	0.0445	0.010	-0.109	-0.056	0.123	-0.008	-0.081
18	23.04	15	0.0833	0.029	0.023	-0.041	0.018	-0.029	-0.137
24	37.10	21	0.0164	0.013	0.127	0.050	-0.111	0.080	0.133
30	42.44	27	0.0298	-0.014	0.062	0.101	0.007	-0.041	0.066
36	45.42	33	0.0734	0.041	-0.033	-0.005	0.015	-0.039	-0.080
42	47.53	39	0.1642	-0.047	0.033	0.030	0.054	-0.014	0.016

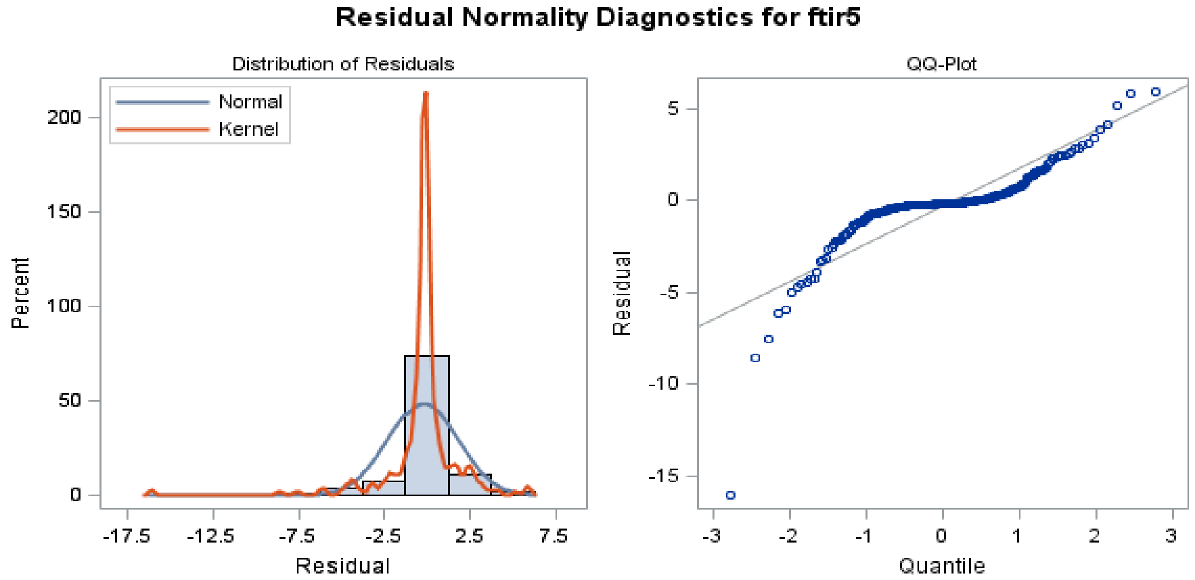

Figure 17. Test on Normality of Error of ARIMA (3,0,0) on Lanthanum Oxide (5%) Doped Lithium Tantalate FTIR Data

To make sure whether the ARIMA (3,0,0) was good enough to predict FTIR pattern on Lanthanum Oxide (5%) Doped Lithium Tantalate, plotting between prediction model value and actual data, and also Mean Absolut Percentage Error (MAPE) and R^2 calculation. The result showed that prediction plot of ARIMA (3,0,0) model (Figure 18) had approximated the its actual data, so the model was good enough to be a prediction. Resulted MAPE from the prediction was 0.292% and the R^2 was 94%.

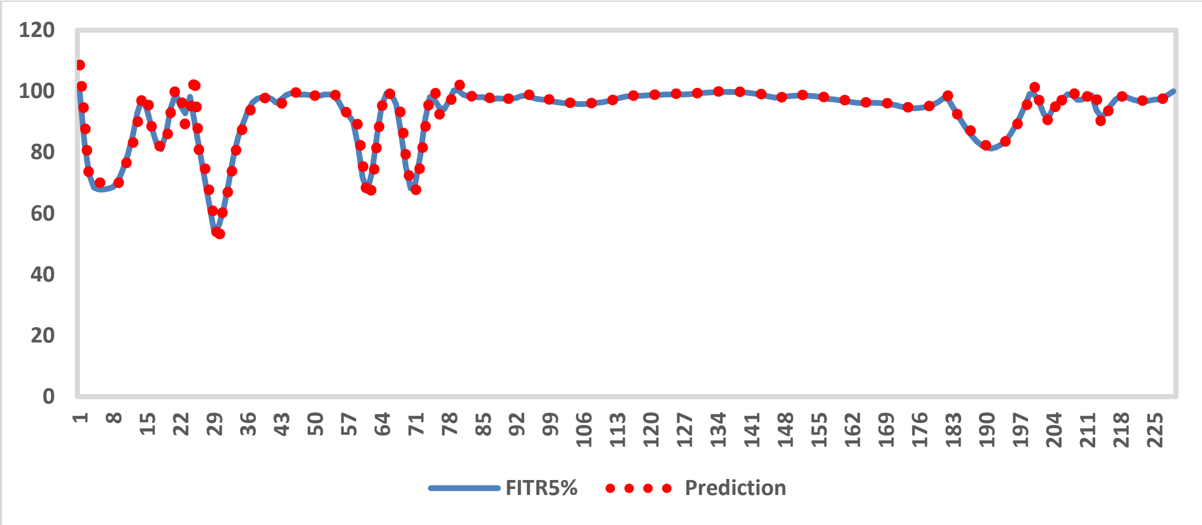

Figure 18. Plot between Actual Data and the Predicted Data of ARIMA (3,0,0) on FITR pattern of Lanthanum Oxide (5%) Doped Lithium Tantalate

From the process above, it could be concluded that FTIR pattern on Lanthanum Oxide (5%) Doped Lithium Tantalate could be well predicted by ARIMA (3,0,0) with the equation model (2):

$$y_t = 108.60558 + 2.06089\, y_{t-1} - 1.59078\, y_{t-2} + 0.51439\, y_{t-3} \quad (2)$$

4.2.3. FTIR Spectrum on thin film of Lanthanum Oxide (10%) doped Lithium Tantalate

Plotting ACF and PACF which showed in Figure 19. Based on ACF and PACF plot, the possible tentative models were ARIMA (3,0,0), ARIMA(2,0,0), ARIMA(1,0,0). To select the best 3 ARIMA models, AIC (Akaike Information Criteria) calculation was done by choosing the smallest AIC. The result was showed Table 11. Model with minimum AIC value was the best model. Based on Table 11, ARIMA model (3,0,0) was the best.

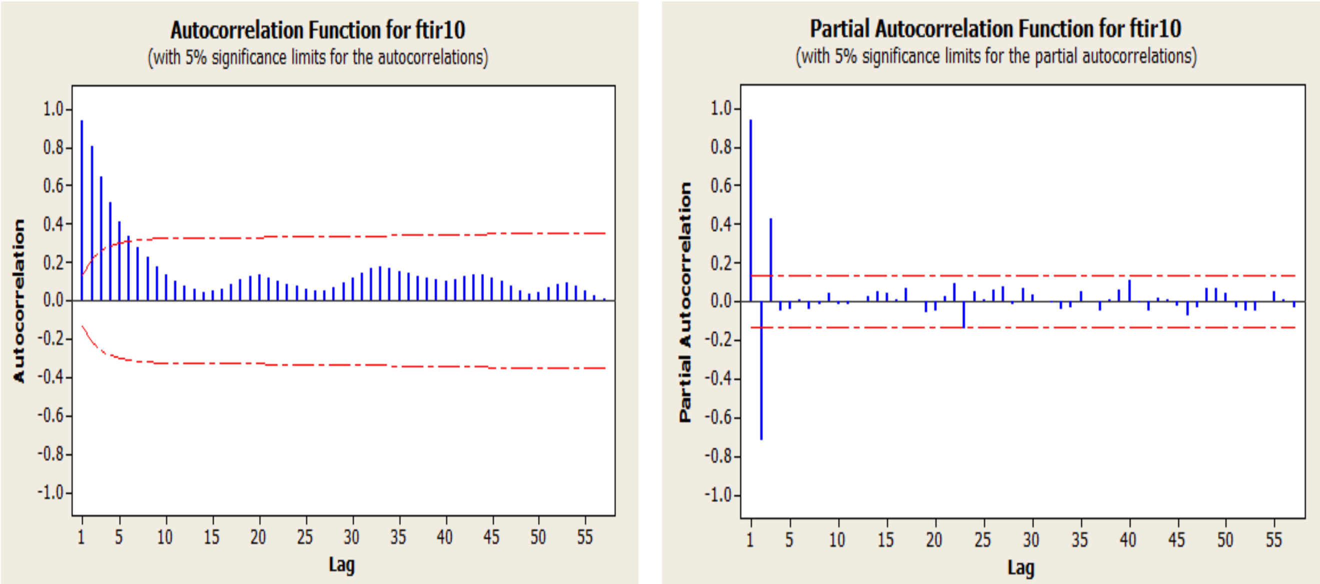

Figure 19. Plot of ACF and PACF on Lanthanum Oxide (10%) Doped Lithium Tantalate FTIR data.

Table 11. AIC value for ARIMA (3,00), ARIMA (2,00) and ARIMA (1,00) Lanthanum Oxide (10%) Doped Lithium Tantalate FTIR Data

Model	AIC
ARIMA (3,0,0)	834.6652
ARIMA (2,0,0)	951.5545
ARIMA (1,0,0)	1134.826

Prediction result of ARIMA (3,0,0) model coefficient showed that all predicted coefficients showed significanct. Model parameters predicted value were showed in Table 12. Based on Table 12, all parameters were significant.

Table 12. ARIMA (3,0,0) Model Coefficient Predicted Value of Lanthanum Oxide (10%) Doped Lithium Tantalate FTIR data

Parameter	Estimate	Standard Error	tValue	ApproxPr>|t|	lag
MU	103.32934	0.87998	117.42	<0.0001	0
AR1,1	2.17493	0.05089	42.74	<0.0001	1
AR1,2	-1.83824	0.09273	-19.82	<0.0001	2
AR1,3	0.64637	0.05090	12.70	<0.0001	3

Based on the ARIMA (3,0,0) model that was pointed above, order combination addition was done on ARIMA (3,0,0) model to get several ARIMA models those were predicted to get the best model. Based on Table 13, ARIMA (3,0,1) model was the best model (lowest AIC). All ARIMA (3,0,1) model coeficients calculation result were significant (Table 14).

Table 13. ARIMA (3,0,0) Model Overfitting on Lanthanum Oxide (10%) Doped Lithium Tantalate FTIR Data

Model	AIC
ARIMA(3,0,0)	834.6652
ARIMA(4,0,0)	811.2258
ARIMA(3,0,1)	800.5630
ARIMA(4,0,1)	802.5547

Table 14. ARIMA (3,0,1) Model Coefficient Prediction Value on Lanthanum Oxide (10%) Doped Lithium Tantalate FTIR Data

Parameter	Estimate	Standard Error	tValue	ApproxPr>|t|	lag
MU	103.43134	0.57541	179.75	<0.0001	0
MA1,1	-0.57862	0.07046	-8.21	<0.0001	1
AR1,1	1.88873	0.07623	24.78	<0.0001	1
AR1,2	-1.35315	0.13704	-9.87	<0.0001	2
AR1,3	0.43409	0.07328	5.92	<0.0001	3

Assumption on ARIMA model was independent residuals and normal distribution. Therefore, ARIMA (3,0,1) model residual was undergone test on independence (Table 15) and normality (Figure 20). The test result showed that ARIMA (3,0,1) model residual was independent and normally distributed (Table and graph below).

Table 15. Test on Independence of Error of ARIMA (3,0,1) on Lanthanum Oxide (10%) Doped Lithium Tantalate FTIR Data

To Lag	Chi-Square	DF	Pr>ChiSq	Autocorrelation					
6	1.96	2	0.3753	0.001	-0.000	-0.017	0.019	0.010	-0.087
12	4.28	8	0.8306	0.052	-0.008	-0.081	-0.001	-0.010	-0.015
18	5.54	14	0.9767	-0.023	-0.038	0.014	0.015	-0.036	0.037
24	14.82	20	0.7868	-0.009	0.183	-0.015	0.036	0.000	0.038
30	15.65	26	0.9443	0.009	0.006	-0.030	-0.016	-0.025	0.035
36	20.16	32	0.9484	0.029	-0.023	0.089	0.078	-0.035	0.000
42	24.21	38	0.9598	-0.021	0.086	-0.002	-0.077	0.027	-0.008

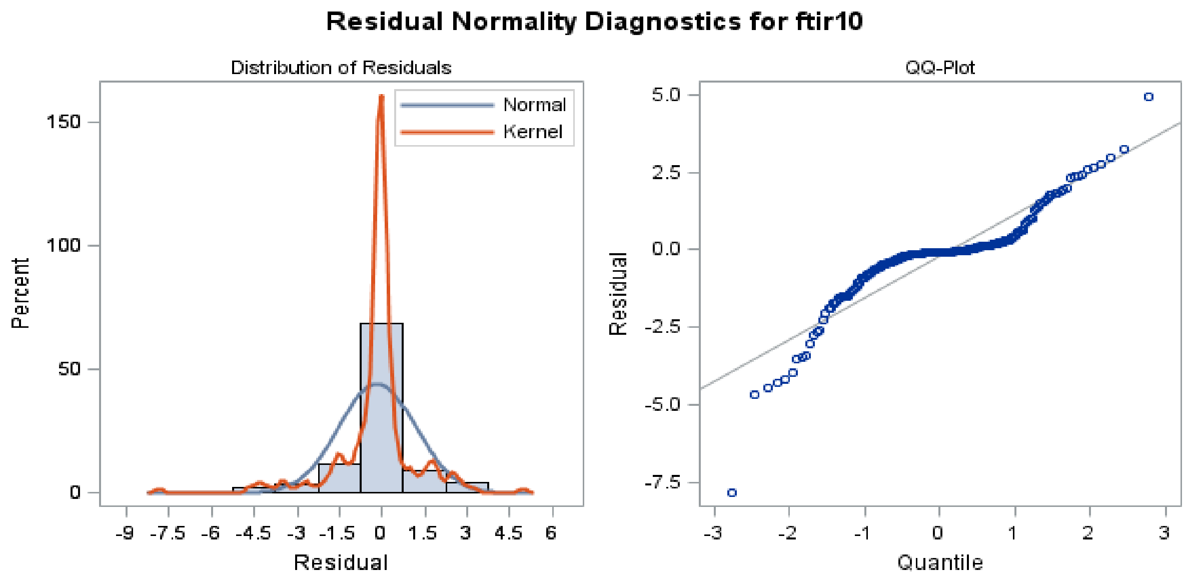

Figure 20. Test on Normality of Error of ARIMA (3,0,1) on Lanthanum Oxide (10%) Doped Lithium Tantalate FTIR Data

To make sure whether the ARIMA (3,0,1) was good enough to predict FTIR pattern on Lanthanum Oxide (10%) Doped Lithium Tantalate, plotting between prediction model value and actual data, and also Mean Absolut Percentage Error (MAPE) and R^2 calculation. The result showed that prediction plot of ARIMA (3,0,1) model (Figure 21) had approximated the its actual data, so the model was good enough to be a prediction. Resulted MAPE from the prediction was 0.876% and the R^2 was 97%.

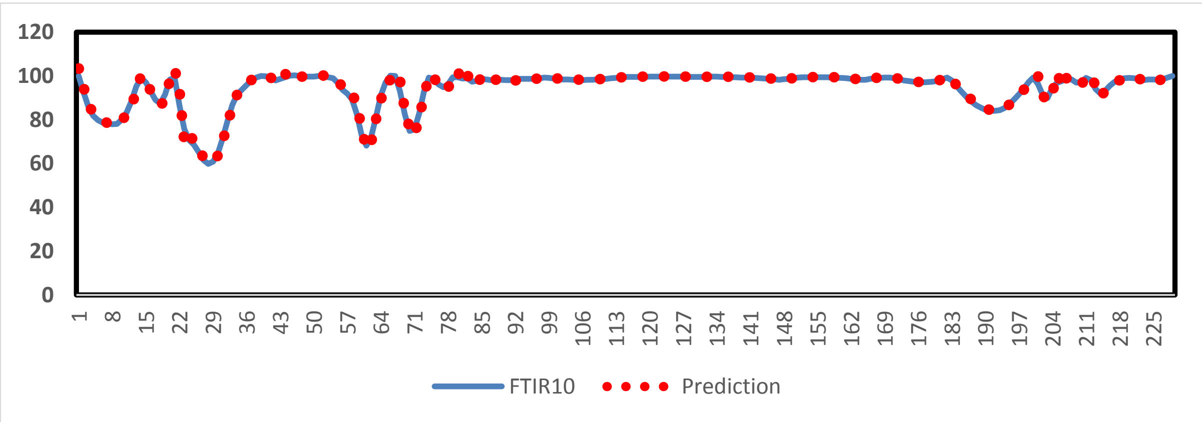

Figure 21. Plot between Actual Data and the Predicted Data of ARIMA (3,0,1) on predicting FITR pattern of Lanthanum Oxide (10%) Doped Lithium Tantalate

From the process above, it could be concluded that FTIR pattern on Lanthanum Oxide (10%) Doped Lithium Tantalate could be well predicted by ARIMA (3,0,1) with the equation model (3):

$$y_t = 103.43134 + 1.88873\, y_{t-1} - 1.35315\, y_{t-2} + 0.43409\, y_{t-3} - 0.57862\, e_{t-1} \qquad (3)$$

4.3. ARIMA on Lithium Tantalate thin film XRD spectrum

Data on Figure 10, 11, 12 were the XRD spectrum data of Lanthanum Oxide (0%, 5%, 10%) doped Lithium Tantalate. The test result with Augmented Dickey-Fuller showed a stationay average. Test result showed with p-value <0.0001 on stationary average. Thus, developed ARIMA models were non-differensing model for XRD data of Lanthanum Oxide (0%, 5%, 10%) doped Lithium Tantalate.

4.3.1. XRD on Lanthanum Oxide (0%) doped Lithium Tantalate

Plotting ACF and PACF for XRD data on Lanthanum Oxide (0%) doped Lithium Tantalate was showed in Figure 22. Based on ACF and PACF plot, the possible tentative models were ARIMA (4,0,0), ARIMA (3,0,0), ARIMA(2,0,0), ARIMA(1,0,0). To select the best from these four ARIMA models, AIC (Akaike Information Criteria) calculation were done by choosing the smallest AIC. The result was showed Table 16. Model with minimum AIC value was the best model. Based on Table 16, ARIMA model (4,0,0) was the best.

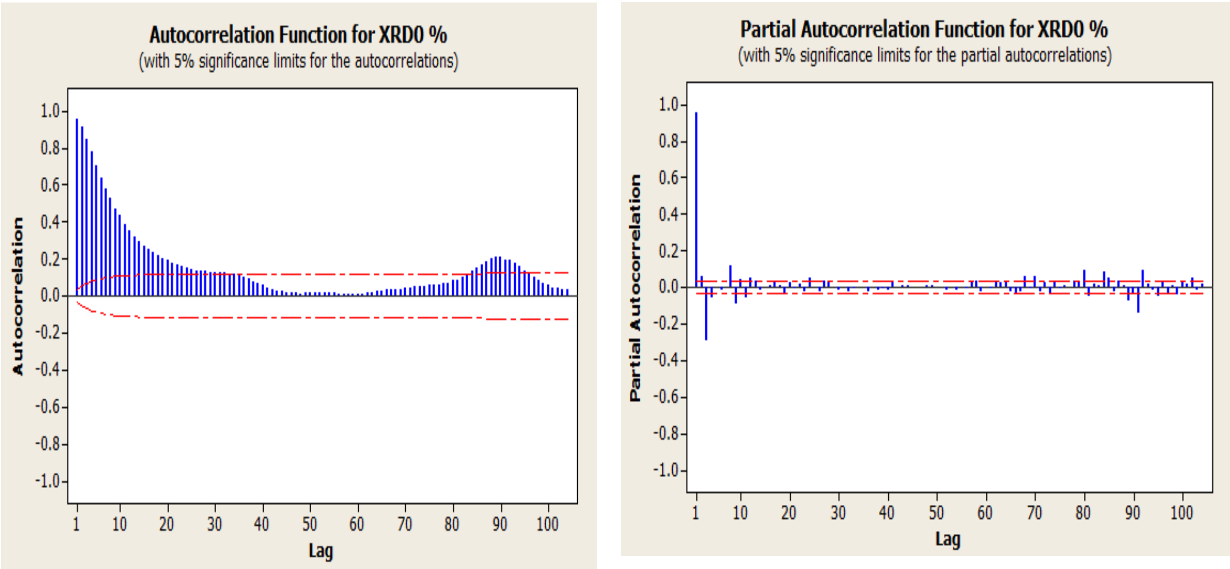

Figure 22. Plot of ACF and PACF on Lanthanum Oxide (0%) Doped Lithium Tantalate XRD data.

Table 16. AIC value for ARIMA (4,0,0), ARIMA (3,00), ARIMA (2,00) and ARIMA (1,00) Lanthanum Oxide (0%) Doped Lithium Tantalate XRD data

Model	AIC
ARIMA (1,0,0)	27944.7
ARIMA (2,0,0)	27936,0
ARIMA (3,0,0)	27623.4
ARIMA (4,0,0)	27613.4

Prediction result of ARIMA (4,0,0) model coefficients showed that all predicted coefficients showed significant. Model parameters predicted value were showed in Table 17. Based on Table 17, all parametera were significant.

Table 17. ARIMA (4,0,0) Model Coefficient Predicted Value of Lanthanum Oxide (0%) Doped Lithium Tantalate XRD data

Parameter	Estimate	Standard Error	tValue	ApproxPr>|t|	lag
MU	26.40280	3.20164	8.25	<0.0001	0
AR1,1	0.89736	0.01688	53.15	<0.0001	1
AR1,2	0.33729	0.02234	15.10	<0.0001	2
AR1,3	-0.23977	0.02234	-10.73	<0.0001	3
AR1,4	-0.05842	0.01689	-3.46	0.0005	4

Based on the ARIMA (4,0,0) model that was pointed above, order combination addition was done on ARIMA (4,0,0) model to get several ARIMA models those were predicted to get the best model. Based on the Table 18, ARIMA (5,0,1) model was the best model (lowest AIC). The ARIMA (5,0,1) coefficients calculation result were all significant (Table 19)

Table 18. ARIMA (4,0,0) Model Overfitting on Lanthanum Oxide (0%) Doped Lithium Tantalate XRD Data

Model	AIC
ARIMA(4,0,0)	27613.41
ARIMA(5,0,0)	27615.39
ARIMA(5,0,1)	27612.92
ARIMA(4,0,1)	27615.37

Table 19. ARIMA (5,0,1) Model Coefficient Prediction Value on Lanthanum Oxide (0%) Doped Lithium Tantalate XRD Data

Parameter	Estimate	Standard Error	tValue	ApproxPr>|t|	lag
MU	24.88538	5.82974	4.27	<0.0001	0
MA1,1	0.99502	0.0059736	166.57	<0.0001	1
AR1,1	1.89167	0.01789	105.73	<0.0001	1
AR1,2	-0.55394	0.03651	-15.17	<0.0001	2
AR1,3	-0.57638	0.03599	-16.01	<0.0001	3
AR1,4	0.17659	0.03617	4.88	<0.0001	4
AR1,5	0.06190	0.01693	3.66	0.0003	5

Assumption on ARIMA model was independent residuals and normal distribution. Therefore, ARIMA (5,0,1) model residual was undergone test on independence (Table 20) and normality (Figure 23). The test result showed that ARIMA (5,0,1) model residual was independent and normally distributed (Table and graph below).

Table 20. Test on Independence of Error of ARIMA (5,0,1) on Lanthanum Oxide (0%) Doped Lithium Tantalate XRD Data

To Lag	Chi-Square	DF	Pr>ChiSq	Autocorrelation					
6		0		-0.001	-0.003	-0.005	0.013	0.042	-0.034
12	112.63	6	<0.0001	-0.085	0.082	-0.044	0.088	-0.074	-0.005
18	130.07	12	<0.0001	0.023	0.004	-0.004	-0.023	-0.012	0.061
24	147.76	18	<0.0001	-0.036	0.028	-0.012	0.031	-0.039	0.016
30	153.54	24	<0.0001	0.013	-0.016	-0.025	0.010	-0.010	0.020
36	157.24	30	<0.0001	0.012	0.015	-0.005	0.012	0.022	-0.006
42	161.19	36	<0.0001	0.007	0.013	0.015	-0.016	-0.013	-0.016
48	163.42	42	<0.0001	-0.010	-0.013	-0.003	-0.010	-0.007	-0.014

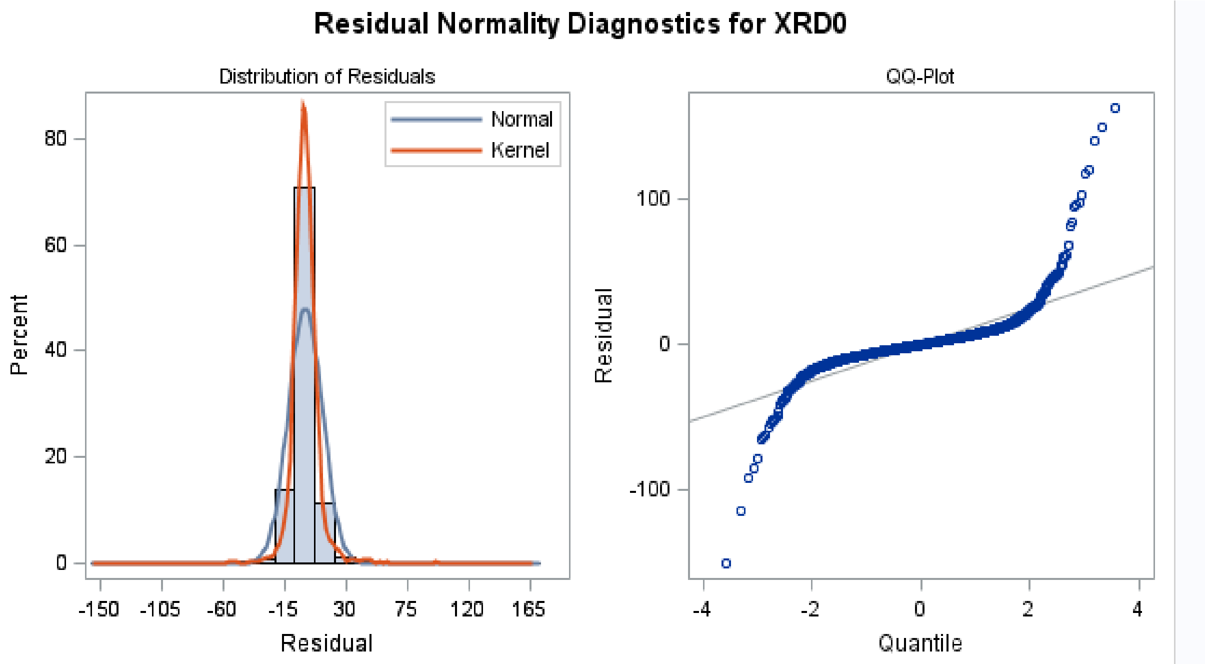

Figure 23. Test on Normality of Error of ARIMA (5,0,1) on Lanthanum Oxide (0%) Doped Lithium Tantalate XRD Data

To make sure whether the ARIMA (5,0,1) good enough to predict XRD pattern on Lanthanum Oxide (0%) Doped Lithium Tantalate, plotting between prediction model value and actual data, and also Mean Absolut Percentage Error (MAPE) and R^2 calculation. The result showed that prediction plot of ARIMA (5,0,1) model (Figure 24) had approximated the its actual data, so the model was good enough to be a prediction. Resulted MAPE from the prediction was 37% and the R^2 was 91%.

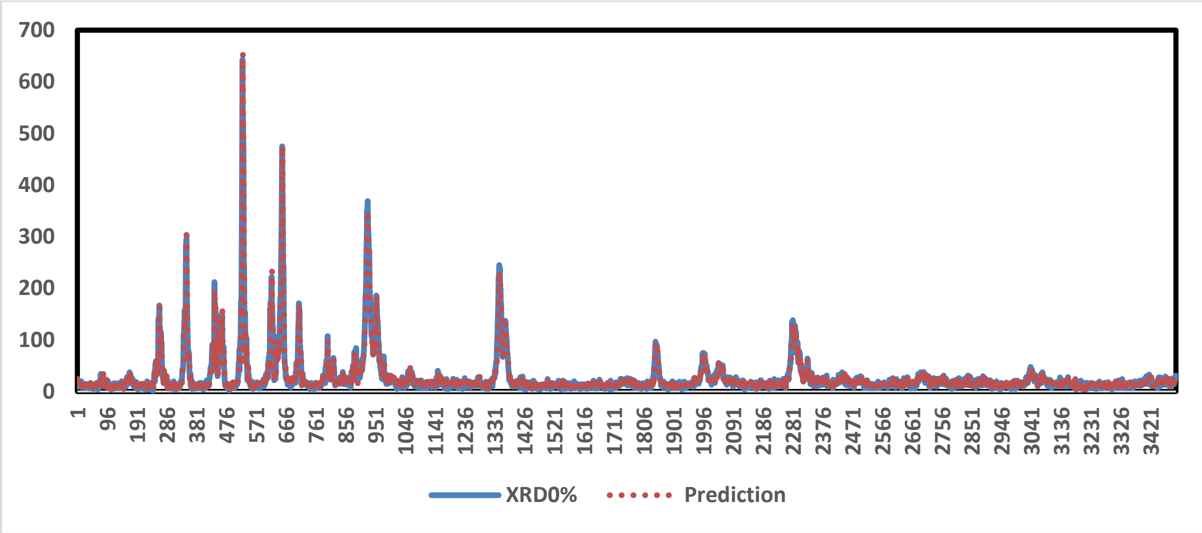

Figure 24. Plot of Actual Data and the Predicted Data of ARIMA (5,0,1) on predicting XRD pattern of Lanthanum Oxide (0%) Doped Lithium Tantalate

From the process above, it could be concluded that XRD pattern on Lanthanum Oxide (0%) doped Lithium Tantalate could be well predicted by ARIMA (5,0,1) model with the equation model below:

$$y_t = 24.88538 + 1.89167\, y_{t-1} - 0.55394\, y_{t-2} - 0.57638\, y_{t-3} \\ +0.17659\, y_{t-4} + 0.06190\, y_{t-5} + 0.99502\, e_{t-1}$$

4.3.2. XRD on Lanthanum Oxide (5%) doped Lithium Tantalate

ACF dan PACF plot for XRD on Lanthanum Oxide (5%) doped Lithium Tantalate was shown in Figure 25. Based on ACF and PACF plot, the possible tentative models were ARIMA (3,0,0), ARIMA(2,0,0), ARIMA(4,0,0), ARIMA (5,0,0). To select the best 3 ARIMA models, AIC (Akaike Information Criteria) calculation was done by choosing the smallest AIC. The result was showed Table 21. Model with minimum AIC value was the best model. Based on Table 21, ARIMA model (3,0,0) was the best.

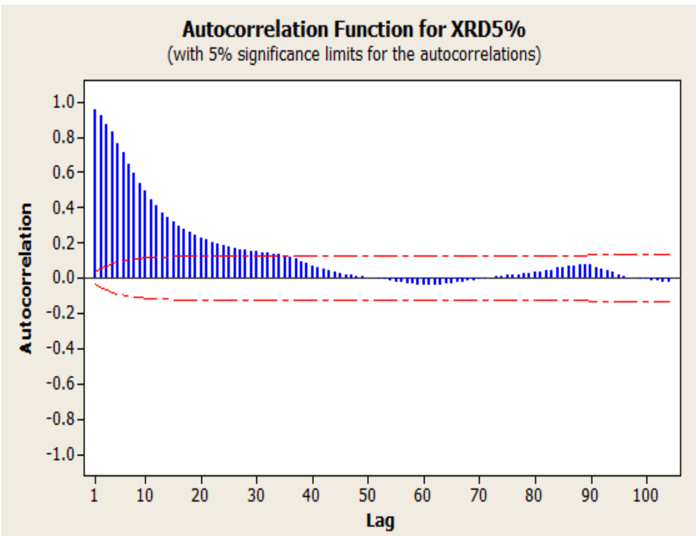

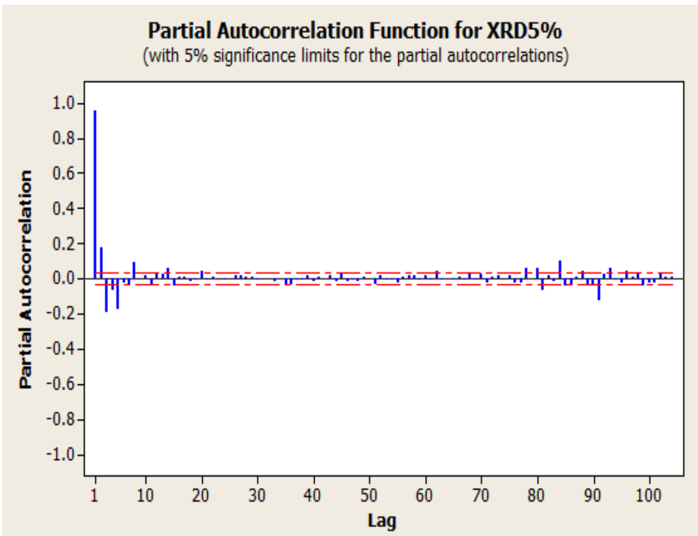

Figure 25. Plot of ACF and PACF on Lanthanum Oxide (5%) Doped Lithium Tantalate XRD data

Table 21. AIC value for ARIMA (2,0,0), ARIMA (3,0,0) , ARIMA (4,00) and ARIMA (5,00) Lanthanum Oxide (5%) Doped Lithium Tantalate XRD Data

Model	AIC
ARIMA (2,0,0)	26582.75
ARIMA (3,0,0)	26449.36
ARIMA (4,0,0)	26433.91
ARIMA (5,0,0)	26331.24

Prediction result of ARIMA (5,0,0) model coefficient showed that all predicted coefficients showed significant. Model parameters predicted value were showed in Table 22. Based on Table 22, all parameters were significant.

Tabel 22. ARIMA (5,0,0) Model Coefficient Predicted Value of Lanthanum Oxide (5%) Doped Lithium Tantalate XRD data

Parameter	Estimate	Standard Error	T_Value	Approx Pt>|t|	Lag
Mu	24.75810	2.82862	8.75	<0.0001	0
AR1,1	0.79374	0.01666	47.63	<0.0001	1
AR1,2	0.32727	0.02137	15.31	<0.0001	2
AR1,3	-0.07677	0.02204	-3.48	0.0005	3
AR1,4	0.06781	0.02137	3.17	0.0015	4
AR1,5	-0.17164	0.01667	-10.30	<0.0001	5

Based on the ARIMA (5,0,0) model that was pointed above, order combination addition was done on ARIMA (5,0,0) model to get several ARIMA models those were predicted to get the best model. Based on Table 23, ARIMA (5,0,1) model was the best model (lowest AIC). All ARIMA (5,0,1) model coeficients calculation result were significant (Table 24).

Tabel 23. ARIMA (5,0,0) Model Overfitting on Lanthanum Oxide (5%) Doped Lithium Tantalate XRS Data

Model	AIC
ARIMA(5,0,0)	26331.24
ARIMA(6,0,0)	26330.84
ARIMA(6,0,1)	26333.31
ARIMA(5,0,1)	26330.35

Tabel 24. ARIMA (5,0,1) Model Coefficient Prediction Value on Lanthanum Oxide (5%) Doped Lithium Tantalate XRD Data

Parameter	Estimate	Standard Error	T_Value	Approx Pr>|t|	Lag
MU	24.77925	2.74304	9.03	<0.0001	0
MA1,1	0.16344	0.09462	1.73	0.0842	1
AR1,1	0.95223	0.09345	10.19	<0.0001	1
AR1,2	0.19954	0.07705	2.59	0.0096	2

AR1,3	-0.13235	0.04053	-3.47	0.0011	3
AR1,4	0.08956	0.02538	3.53	0.0004	4
AR1,5	-0.16052	0.01903	-8.43	<0.0001	5

Assumption on ARIMA model was independent residuals and normal distribution. Therefore, ARIMA (5,0,1) model residual was undergone test on independence (Table 25) and normality (Figure 26). The test result showed that ARIMA (5,0,1) model residual was independent and normally distributed (Table and graph below).

Table 25. Test on Independence of Error of ARIMA (5,0,1) on Lanthanum Oxide (5%) Doped Lithium Tantalate XRD Data

To Lag	Chi-Square	DF	Pr>ChiSq	Autocorrelation					
6		0		-0.000	-0.002	0.014	0.001	0.023	0.005
12	39.47	6	<0.0001	-0.079	0.024	-0.003	0.037	-0.044	-0.019
18	64.30	12	<0.0001	-0.036	0.064	-0.025	0.005	0.021	0.023
24	76.44	18	<0.0001	-0.025	0.038	-0.014	0.028	0.012	0.018
30	77.82	24	<0.0001	-0.014	0.006	-0.007	0.009	0.002	-0.004
36	89.94	30	<0.0001	-0.001	0.016	-0.005	0.048	0.023	0.017
42	92.80	36	<0.0001	0.011	0.004	0.015	-0.002	-0.015	-0.014
48	97.43	43	<0.0001	0.005	-0.025	0.013	-0.008	0.003	-0.021

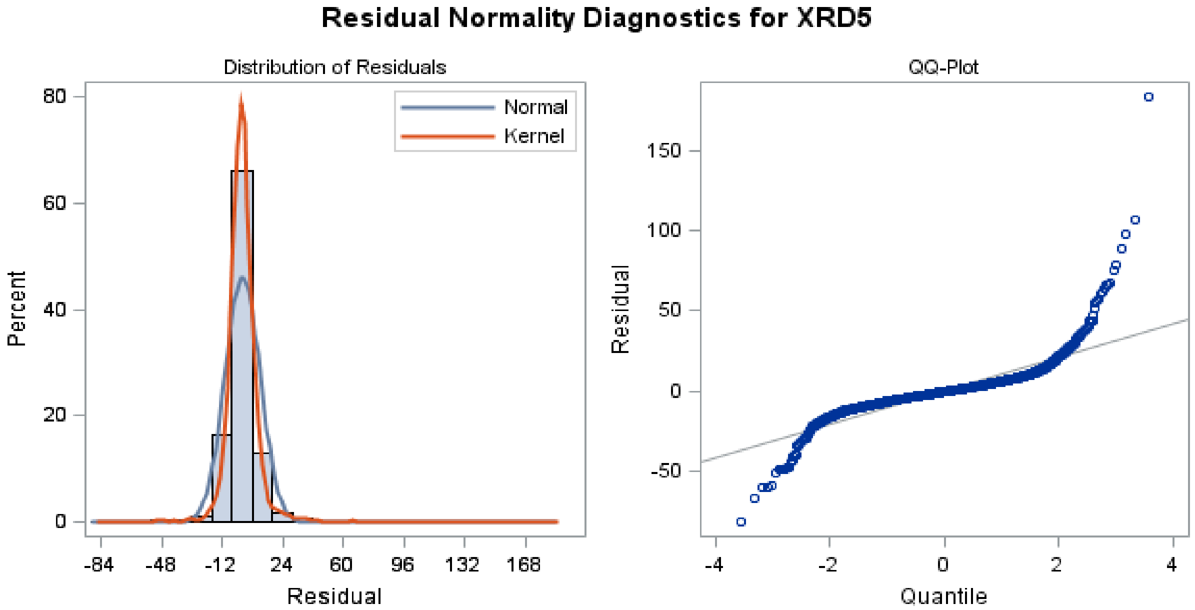

Figure 26. Test on Normality of Error of ARIMA (5,0,1) on Lanthanum Oxide (5%) Doped Lithium Tantalate XRD Data

To make sure whether the ARIMA (5,0,1) good enough to predict XRD pattern on Lanthanum Oxide (5%) Doped Lithium Tantalate, plotting between prediction model value and actual data, and also Mean Absolut Percentage Error (MAPE) and R^2 calculation. The result showed that prediction plot of ARIMA (5,0,1) model (Figure 27) had approximated the its actual data, so the model was good enough to be a prediction. Resulted MAPE from the prediction was 35% and the R^2 was 92%.

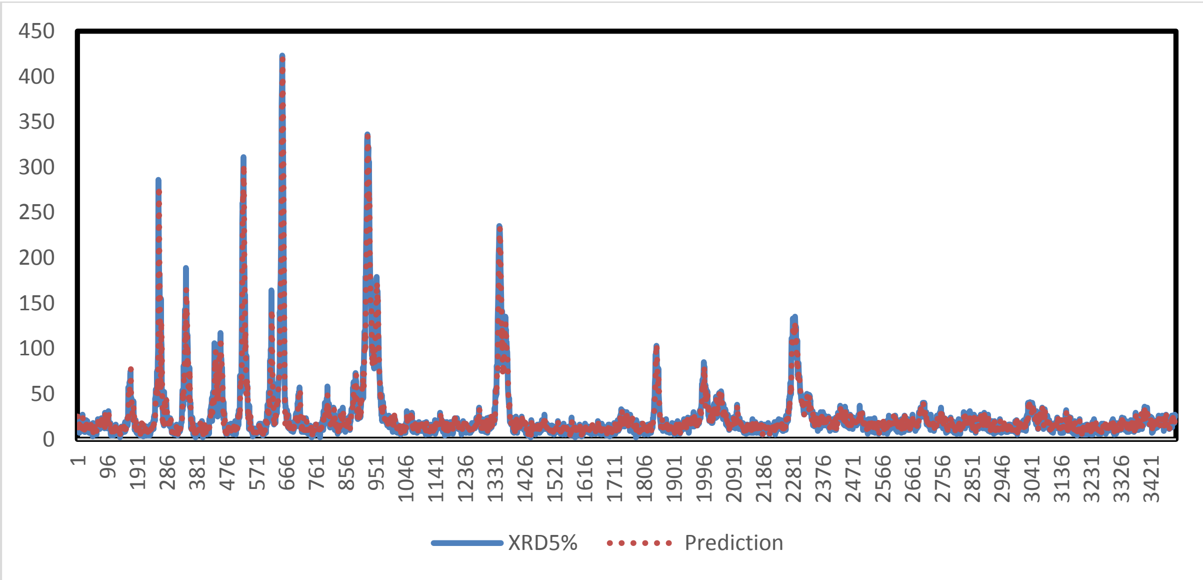

Gambar 27. Plot of Actual Data and the Predicted Data of ARIMA (5,0,1) on predicting XRD pattern of Lanthanum Oxide (5%) Doped Lithium Tantalate

From the process above, it could be concluded that XRD pattern on Lanthanum Oxide (5%) Doped Lithium Tantalate could be well predicted by ARIMA (5,0,1) with the equation model (5):

$$y_t = 24.77925 + 0.95223\, y_{t-1} + 0.19954\, y_{t-2} - 0.13235\, y_{t-3} + 0.08956\, y_{t-4} - 0.08956\, y_{t-5} + 0.16344\, e_{t-1} \quad (5)$$

4.3.3. XRD pada Lanthanum Oksida (10 %) Doped Lithium Tantalat

ACF dan PACF plot for XRD on Lanthanum Oxide (10%) doped Lithium Tantalate was shown in Figure 28. Based on ACF and PACF plot, the possible tentative models were ARIMA (3,0,0), ARIMA(4,0,0), ARIMA(5,0,0), ARIMA (7,0,0). To select the best 3 ARIMA models, AIC (Akaike Information Criteria) calculation was done by choosing the smallest AIC. The result was showed Table 26. Model with minimum AIC value was the best model. Based on Table 26, ARIMA model (7,0,0) was the best.

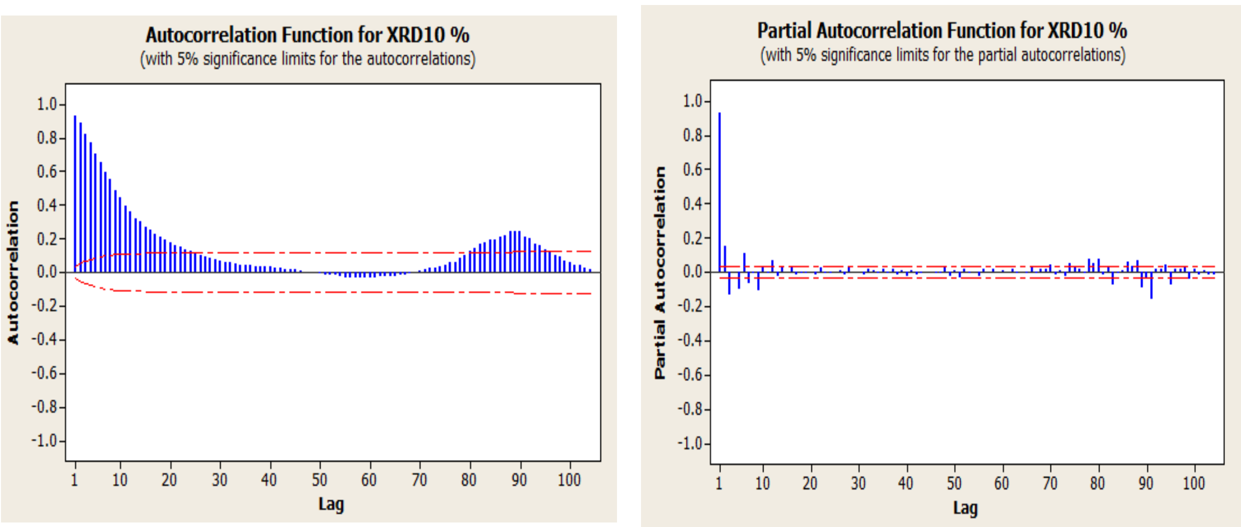

Gambar 28. Plot of ACF and PACF on Lanthanum Oxide (10%) Doped Lithium Tantalate XRD data

Tabel 26. AIC value for ARIMA (3,0,0), ARIMA (4,0,0) , ARIMA (5,00) and ARIMA (7,00) Lanthanum Oxide (10%) Doped Lithium Tantalate XRD Data

Model	AIC
ARIMA (3,0,0)	25824.27
ARIMA (5,0,0)	25794.36
ARIMA (4,0,0)	25755.70
ARIMA (7,0,0)	25740.54

Prediction result of ARIMA (7,0,0) model coefficient showed that all predicted coefficients showed significant. Model parameters predicted value were showed in Table 27. Based on Table 27, all parameters were significant.

Tabel 27. ARIMA (7,0,0) Model Coefficient Predicted Value of Lanthanum Oxide (10%) Doped Lithium Tantalate XRD data

Parameter	Estimate	Standard Error	T_Value	Approx Pt>|t|	Lag
MU	19.83223	2.19020	9.06	<0.0001	0
AR1,1	0.82856	0.01688	49.08	<0.0001	1
AR1,2	0.22276	0.02177	10.23	<0.0001	2
AR1,3	-0.09296	0.02190	-4.24	<0.0001	3
AR1,4	0.04381	0.02195	2.00	0.0460	4
AR1,5	-0.16876	0.02191	-7.70	<0.0001	5
AR1,6	0.16489	0.02177	7.68	<0.0001	6
AR1,7	-0.06993	0.01688	-4.14	<0.0001	7

Based on the ARIMA (7,0,0) model that was pointed above, order combination addition was done on ARIMA (7,0,0) model to get several ARIMA models those were predicted to get the best model (Table 28). Based on Table 28, ARIMA (8,0,1) model was the best model (lowest AIC). ARIMA (8,0,1) model coeficient calculation result were not all significant (Table 29).

Tabel 28. ARIMA (7,0,0) Model Overfitting on Lanthanum Oxide (10%) Doped Lithium Tantalate XRD Data

Model	AIC
ARIMA(7,0,0)	25740.54
ARIMA(8,0,0)	25742.44
ARIMA(8,0,1)	25697.63
ARIMA(7,0,1)	25736.56

Tabel 29. ARIMA (8,0,1) Model Coefficient Prediction Value on Lanthanum Oxide (10%) Doped Lithium Tantalate XRD Data

Parameter	Estmate	Standard Error	T Value	Approx Pr>|t|	Lag
MU	19.79149	2,21258	8.94	<0.0001	0
MA1,1	-0.99122	0.0035032	-282.95	<0.0001	1
AR1,1	-0.14798	0.01729	-8,56	<0.0001	1

AR1,2	1.02974	0.01735	59.35	<0.0001	2
AR1,3	0.12821	0.02438	5.26	<0.0001	3
AR1,4	-0.04792	0.02439	-1.96	0.0495	4
AR1,5	-0.12397	0.02439	-5.08	<0.0001	5
AR1,6	-0.0046989	0.02438	-0.19	0.8472	6
AR1,7	0.07459	0.01723	4.33	<0.0001	7
AR1,8	-0.04819	0.01710	-2.82	0.0049	8

One ARIMA (8,0,1) model coefficient was not significant on alpha 5%, thus ARIMA (7,0,0) model was selected instead. Assumption on ARIMA model was independent residuals and normal distribution. Therefore, ARIMA (7,0,0) model residual was undergone test on independence (Table 30) and normality (Figure 29). The test result showed that ARIMA (7,0,0) model residual was independent and normally distributed (Table and graph below).

Table 30. Test on Independence of Error of ARIMA (7,0,0) on Lanthanum Oxide (10%) Doped Lithium Tantalate XRD Data

To Lag	Chi-Square	DF	Pr>ChiSq	Autocorrelation					
6		0		-0.001	-0.0.02	0.006	-0.008	-0.003	-0.009
12	35.43	3	<0.0001	0.039	0.073	-0.028	-0.011	-0.046	0.006
18	42.21	9	<0.0001	-0.038	-0.004	-0.014	0.011	0.010	-0.005
24	45.02	15	<0.0001	0.009	-0.001	-0.017	0.005	0.016	-0.012
30	47.40	21	0.0008	0.011	0.005	-0.018	-0.005	0.012	0.006
36	54.00	27	0.0015	-0.011	-0.010	0.013	-0.025	0.014	-0.026
42	69.41	33	0.0002	0.029	-0.020	0.032	-0.024	0.034	-0.018
48	80.58	39	0.0001	0.015	-0.028	0.038	-0.025	0.006	-0.005

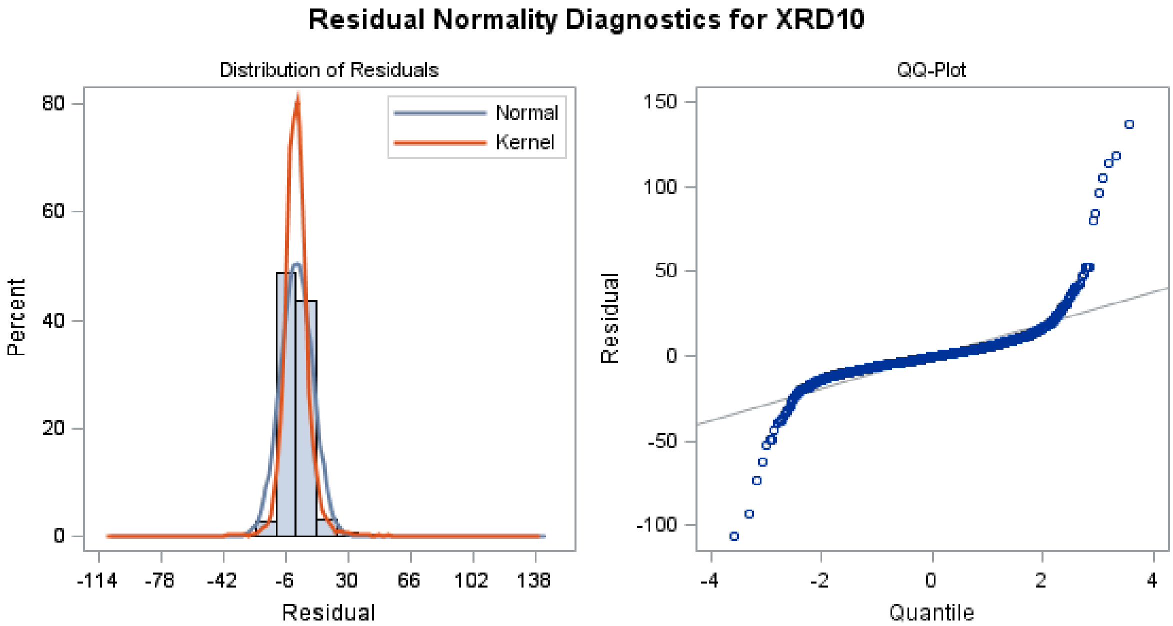

Figure 29. Test on Normality of Error of ARIMA (7,0,0) on Lanthanum Oxide (10%) Doped Lithium Tantalate XRD Data

To make sure whether the ARIMA (7,0,0) good enough to predict XRD pattern on Lanthanum Oxide (10%) Doped Lithium Tantalate, plotting between prediction model value and actual data, and also Mean Absolut Percentage Error (MAPE) and R^2 calculation. The result showed that prediction plot of ARIMA (7,0,0) model (Figure 30) had approximated the its actual data, so the model was good enough to be prediction. Resulted MAPE from the prediction was 38% and the R^2 was 87%.

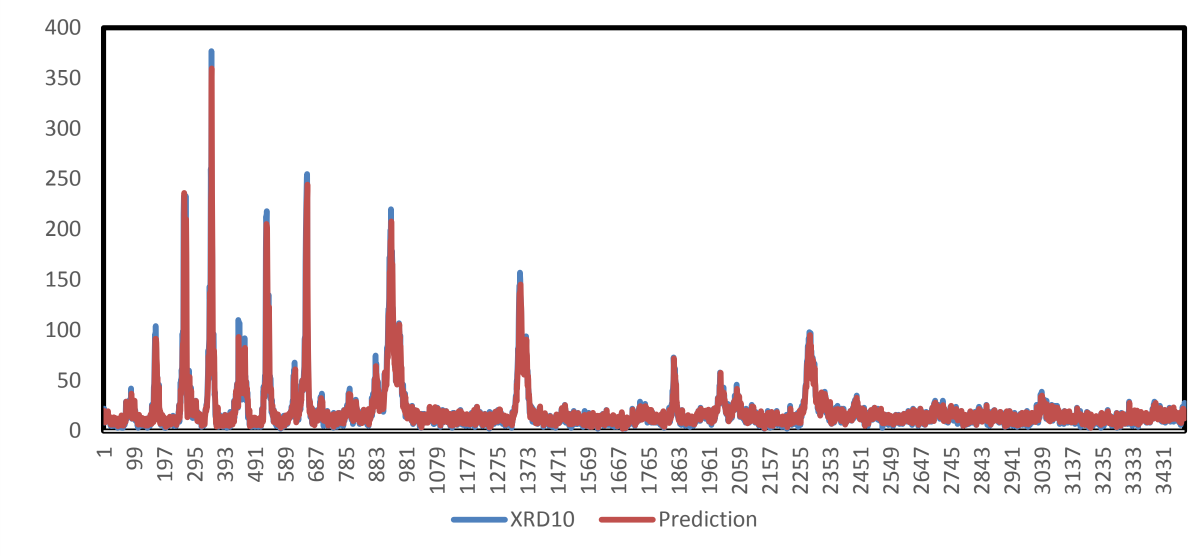

Gambar 30. Plot of Actual Data and the Predicted Data of ARIMA (7,0,0) on predicting XRD pattern of Lanthanum Oxide (10%) Doped Lithium Tantalate

From the process above, it could be concluded that XRD pattern on Lanthanum Oxide (10%) Doped Lithium Tantalate could be well predicted by ARIMA (7,0,0) with the equation model below:

$$y_t = 19.83223 + 0.82856\, y_{t-1} + 0.22276\, y_{t-2} - 0.09296\, y_{t-3} + 0.04381\, y_{t-4} - 0.16876\, y_{t-5} + 0.16489\, y_{t-6} - 0.06993\, y_{y-7}$$

4.4. Effect of Lanthanum Oxide doped to the Lithium Tantalate FTIR

Analysis of effect of Lanthanum oxide doped to the Lithium Tantalate FTIR was done through coupled observasion. Control FTIR value (0% Lanthanum Oxide doped Lithium Tantalate) was coupled with FTIR value of the Lanthanum oxide (5% and 10%) doped Lithium Tantalate. The hope was for the difference was around zero.

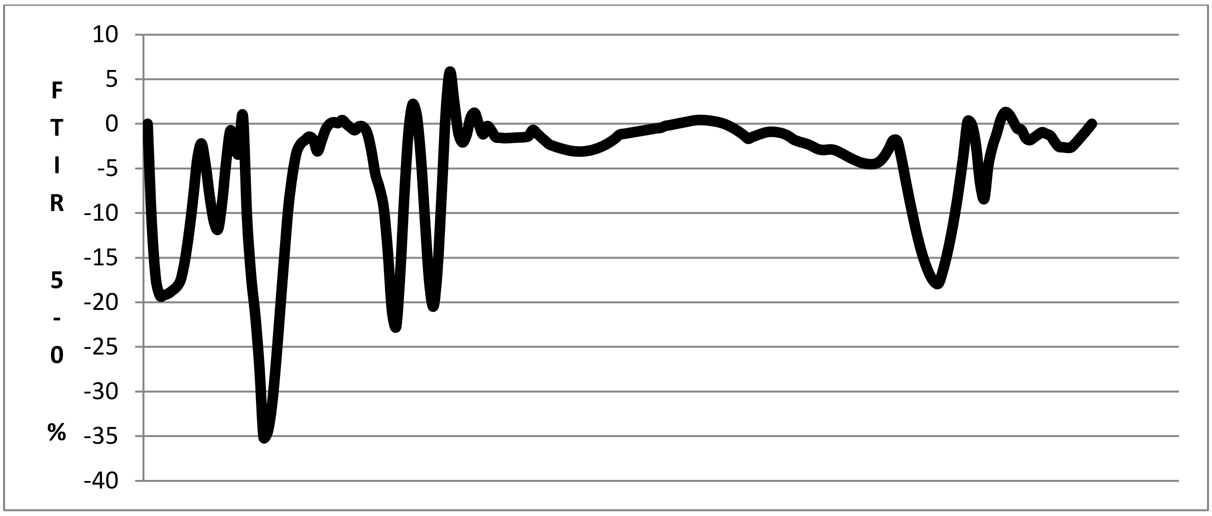

Figure 31. Difference data plot between FTIR value of Lanthanum Oxide (5%) doped Lithium Tantalate with the Control FTIR value.

From the Figure 31, it could be suggested that the difference data between FTIR value of Lanthanum Oxide (5%) doped Lithium Tantalate with the Control FTIR value usually below zero with several point much below zero, with the average difference data of -4.79194. This showed that Lanthanum Oxide (5%) doped Lithium Tantalate would decrease the FTIR value. From statistic test with $t_{\text{-compute}}$, it could get value -10.4541. Meanwhile t-table with alfa 5% was equal to -2.26 which means difference data plot between FTIR value of Lanthanum Oxide (5%) doped Lithium Tantalate with the Control FTIR value was not zero or; in other words, 5% doped by Lanthanum Oxide could decrease FTIR value.

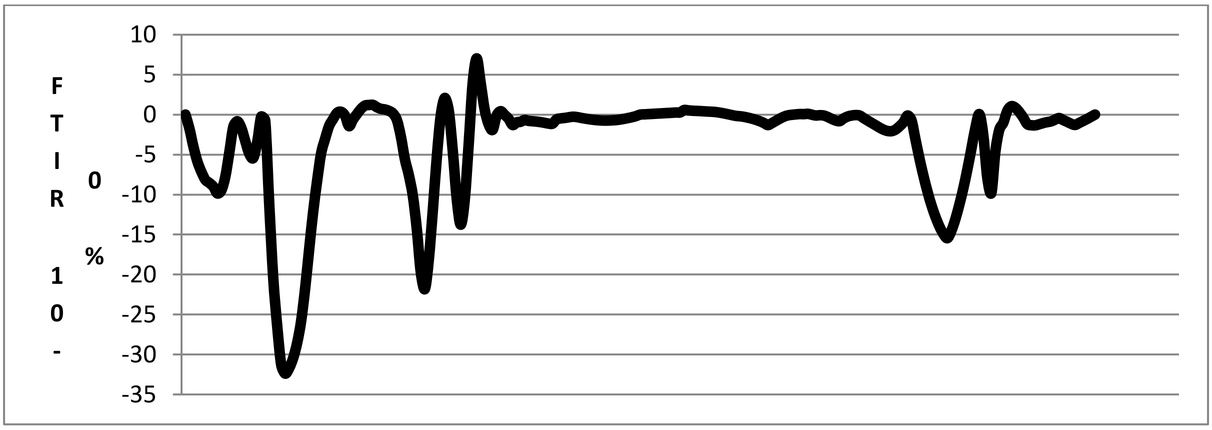

Figure 32. Difference data plot between FTIR value of Lanthanum Oxide (10%) doped Lithium Tantalate with the Control FTIR value.

From the Figure 32, it could be suggested that the difference data between FTIR value of Lanthanum Oxide (10%) doped Lithium Tantalate with the Control FTIR value usually below zero with several point much below zero, with the average difference data of -3.43758. This showed that Lanthanum Oxide (10%) doped Lithium Tantalate would decrease the FTIR value. From statistic test with $t_{\text{-compute}}$, it could get value -7.83734. Meanwhile t-table with alfa 5% was equal to -2.26 which means difference data plot between FTIR value of Lanthanum Oxide (10%) doped Lithium Tantalate with the Control FTIR value was not zero or; in other words, 10% doped by Lanthanum Oxide could decrease FTIR value.

4.5. Effect of Lanthanum Oxide doped to the Lithium Tantalate XRD

Analysis of effect of Lanthanum oxide dopde to the Lithium Tantalate XRD was done through coupled observation. Control XRD value (0% Lanthanum Oxide doped Lithium Tantalate) was coupled with XRD value of the Lanthanum oxide (5% and 10%) doped Lithium Tantalate. The hope was for the difference was around zero.

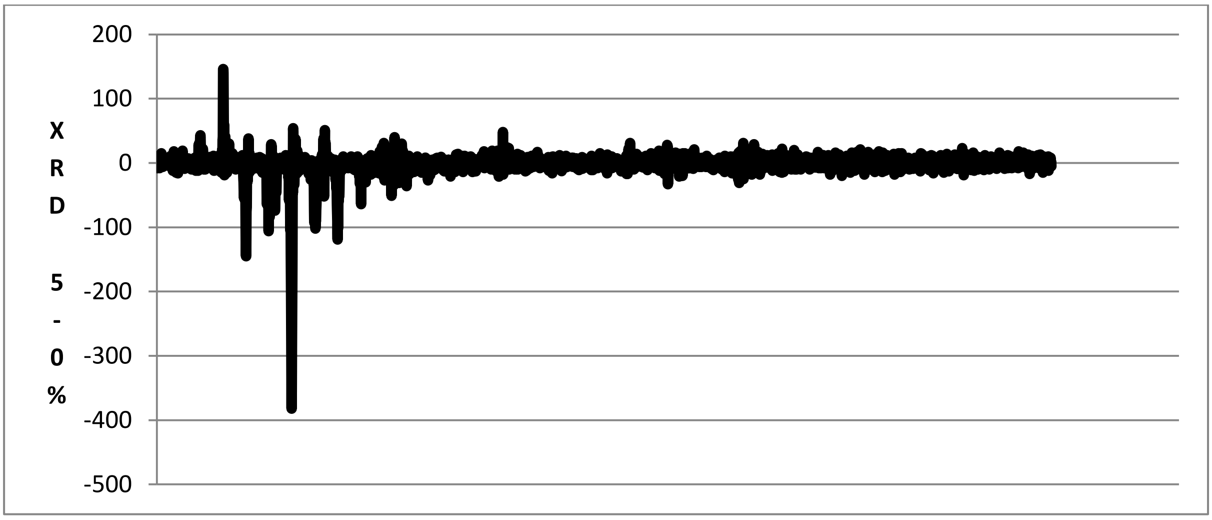

Figure 33. Difference data plot between FTIR value of Lanthanum Oxide (5%) doped Lithium Tantalate with the Control FTIR value.

From the Figure 33, it could be suggested that the difference data between XRD value of Lanthanum Oxide (5%) doped Lithium Tantalate with the Control XRD value is arround zero but several point much below zero, with the average difference data of -1.66381. This showed that Lanthanum Oxide (5%) doped Lithium Tantalate would decrease the XRD value. From statistic test with $t_{\text{-compute}}$, it could get value -5.79336. Meanwhile t-table with alfa 5% was equal to -1.96 which means difference data plot between XRD value of Lanthanum Oxide (5%) doped Lithium Tantalate with the Control XRD value was not zero or; in other words, 5% doped by Lanthanum Oxide could decrease XRD value.

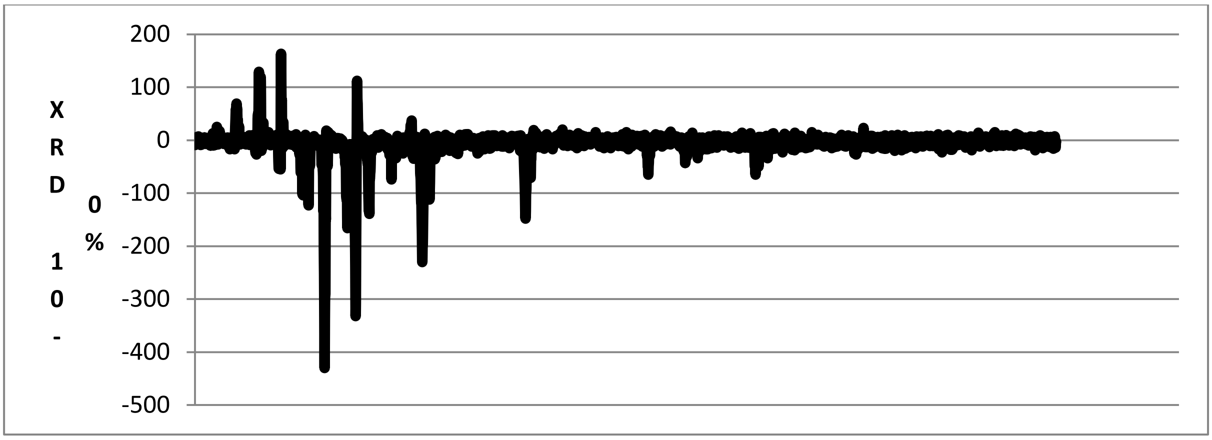

Figure 34. Difference data plot between XRD value of Lanthanum Oxide (10%) doped Lithium Tantalate with the Control XRD value.

From the Figure 34, it could be suggested that the difference data between XRD value of Lanthanum Oxide (10%) doped Lithium Tantalate with the Control XRD value usually arround zero with several point much below zero, with the average difference data of -6.54185. This showed that Lanthanum Oxide (10%) doped Lithium Tantalate would decrease the XRD value. From statistic test with $t_{\text{-compute}}$, it could get value -14.816. Meanwhile t-table with alfa 5% was equal to -1.96 which means difference data plot between FTIR value of Lanthanum Oxide (10%) doped Lithium Tantalate with the Control XRD value was not zero or; in other words, 10% doped by Lanthanum Oxide could decrease XRD value.

V. Conclusion

a) ARIMA model could explain FTIR value pattern and XRD value pattern of Lanthanum Oxide (0%. 5 %, 10 %) doped Lithium Tantalate. This was proven by the R^2 value of ARIMA model which was above 80% and also the prediction pattern of ARIMA model which had approximated the actual data.
b) Coefficient of Determination (R^2) of ARIMA model for Lanthanum Oxide (0%. 5 %, 10 %) doped Lithium Tantalate FTIR were 94%, 94% and 97%, respectively. Coefficient of Determination (R^2) of ARIMA model for Lanthanum Oxide (0%. 5 %, 10 %) doped Lithium Tantalate XRD were 91%, 92% and 87%, respectively.
c) ARIMA models classify XRD and FTIR data to autoregression non differencing models. ARIMA model for Lanthanum Oxide (0%. 5 %, 10 %) doped Lithium Tantalate FTIR were ARIMA (3,0,1), ARIMA (3,0,0), ARIMA (3,0,). ARIMA model for Lanthanum Oxide (0%. 5 %, 10 %) doped Lithium Tantalate XRD were ARIMA (5,0,1), ARIMA (5,0,1), and ARIMA (7,0,0)
d) Accuracy of ARIMA model for Lanthanum Oxide (0%. 5 %, 10 %) doped Lithium Tantalate FTIR was better than the ARIMA model for Lanthanum Oxide (0%. 5 %, 10 %) doped Lithium Tantalate XRD. This was due to ARIMA model of FTIR data was much simpler and had lower MAPE and higher Coefficient of Determination (R^2) compared to ARIMA model of XRD data.
e) Lithium Tantalate doping with Lanthanum Oxide up to 5% and 10% could decrease the FTIR and contol XRD value.

VI. Acknowledgement

This work was supported by Penelitian Unggulan Divisi (PUD), Ministry of Research, Technology, and Higher Education; Republic of Indonesia No. 011/SP2H/LT/DRPM/IV/2017. Thanks also to the Indonesian Government who had given the chance for the authors to conduct this research.

VII. REFERENCES

[1]. Aguas M and Parkin IP (2001) Combined Combustion Sol Gel Syntesis of $LiNbO_3$, $LiTaO_3$, $NaNbO_3$,and $NaTaO_3$. Journal of Material Science Letters 20: 57–58

[2]. Aidi, M.N and Irzaman (2017) ARIMA Analysis For Detecting FTIR And XRD Spectral Pattern on Barium Strontium Titanate (BST) Thin Film. *Submitted to* Spectroscopy and Spectral Analysis

[3]. Aidi MN, Masjkur M, Siswadi, Pramudito S, Arif A, Syafutra H, Alatas H, dan Irzaman (2013) Phase Transformation of Ba0.55Sr0.45TiO3 Tetragonal to Pseudotetragonal Structures and Arima Model for XRD Data. International Journal of Statistic and Application 3 (5): 169-187

[4]. Althowibi JFA (2017) Dynamical X-Ray Diffraction Analysis of Triple-Junction Solar Cells on Germanium (001) Substrates. International Journal of High Speed Electronics and Systems 26: 13

[5]. Anokhina AS, Razumnayaa AG, Yuzyuka YI, Golovko YI and Mukhortov VM (2016) Phase Transitions in Barium–Strontium Titanate Films on MgO Substrates with Various Orientations. Physics of the Solid State 58(1): 2027-2034

[6]. Asadchikov, Buzmakova AV (2009) Laboratory x ray mikrotomograph. ISSN

[7]. Barbieri L (2005) Cathode ray tube glass recycling :an example of clean technology. Waste Management Research ISSN

[8]. Bartasyte A, Margueron S and Baron T (2017) Toward High Quality Epitaxial $LiNbO_3$ and $LiTaO_3$ Thin Films for Acoustic and Optical Applications

[9]. Benzaouak A, Touach N, Ortiz-Martınez VM, Salar-Garcıa MJ, Hernandez-Fernandez FJ, Rıos AP and Mahi ME (2017) Ferroelectric LiTaO3 as Novel Photo-Electro catalystin Microbial Fuel Cells. Environmental Progress and Sustainable Energy 10 (2): 1-7

[10]. Bijay KB, Swonal SD, Avinash M and Partha S (2017) Preparation and Micro structura lCharacterization of Niobium Pentoxide Doped Barium Strontium Titanate Glass and Glass-Ceramics. Trans. Ind. Ceram. Soc. 76 (1): 21-30

[11]. Chang YC, Chen YC, Kao KS, Cheng CC, Chang CC, Shih WC, Lin SH and Lin JM (2017) Deposition of AlN thin films on $LiTaO_3$ substrates. IEEE International Conference on Applied System Innovation 4
[12]. Chowdhurya MKS (2017) Influence of crystal structure on dielectricproperties of Barium Strontium Titanate during high energy ball milling. Materials Today: Proceedings 4: 5631–5639
[13]. Coleman PS, Tschopp MA, Christopher R, Douglas WE (2015) Bridging atomistic simulations and experiments via virtual diffraction: understanding homophase grain boundary and heterophase interface structures. J Mater Sci
[14]. Damodaran AR, Agar JC and Pandya S (2016) New Modalities of Strain-Control of Ferro electric Thin Films. IOP Publishing
[15]. Darmasetiawan H, Irzaman, Indro MN, Sukaryo SG, Hikam M, and Bo NP (2002) Optical Properties of Crystalline Ta_2O_5 Thin Films. phys. stat. sol. (a) 193(1): 53–60
[16]. De´gerine S and Lambert-Lacroix S. Characterization of the partial autocorrelation function of nonstationary time series. Journal of Multivariate Analysis 87: 46-59
[17]. Dickey, DA and Fuller WA (1979) Distribution of the estimators for autoregressive time series with a unit root. Journal of the American Statistical Association 74: 427–431
[18]. Ding A, Xu J, Huang C, Zhou W, Zhao L, Sun J and Wang Q (2017) Synthesis and magneto electric properties of multiferroic composites of lead lanthanum zirconate titanate and meso porous cobalt ferrite. Scripta Materialia 136: 29-32
[19]. Donativi M, Quarta S, Cesareo R, Castellano A (2007) Rayleigh to Compton ratio with mono chromatic radiation from an X-ray tube (preliminary results). Elsevier
[20]. Du H, Jia CL and Mayer J (2015) Surface Atomic Structure and Growth Mechanism of Monodisperse {1 0 0}-Faceted Strontium Titanate Zirconate Nanocubes. Chemistry of Material 1-7
[21]. Dzunuzovic A, Petrovic M, Stojadinovic B, Ilic N, Bobic J, Foschini C, Zaghete M and Stojanovic B (2015) Multiferroic (NiZn) Fe_2O_4 - $BaTiO_3$ composites prepared from nanopowders byauto-combustion method. Ceramics International 1-52
[22]. Edwards PG (2017) Electrical characterization of $LiTaO_3$:P(VDF–TrFE)composites. Springer 6
[23]. Elmaleh MS. ARIMA Forecasting: Variables without a Cause. J. Bus. Val. Econ. Loss Anal. 12(1): 141–143
[24]. Garten LM, Matthew B, Arnab SG, Ryan H, Venkataraman G, Elizabeth CD and Susan TM (2016) Relaxor Ferroelectric Behavior in Barium Strontium Titanate. J. Am. Ceram. Soc 99 (5): 1645-1650
[25]. George B and Gwilym J (1970) Time Series Analysis: Forecasting and Control. San Francisco: Holden-Day 1970.
[26]. Gorelik VS, Sidorov NV and Vodchits AI (2017) Optical Proporties of Lithium Niobate and Lithium Tantalate with Impurities and Defects. Physics of Wave Phenomen 25(1): 10-19
[27]. Hana P, Wang PX, Zhang SY and D. H. Zhu DH (2010) Drought forecasting based on the remote sensing data using ARIMA models. Mathematical and Computer Modelling 51 1398-1403
[28]. Hiranaga Y, Uda T, Kurihashi Y, Tochishita H and Kadota M (2009) Nanodomain Formation on Ferroelectrics and Development of Hard-Disk-Drive-Type Ferroelectric Data Storage Devices. Japanesse Journal of Applied Physics
[29]. Ianculescu AC, Vasilescu CA, Crisan M, Raileanu M, Vasile BS, Calugaru M, Crisan D, Dragan N, Curecheriu L and Mitoseriu L (2015) Formation mechanism and characteristics oflanthanum-doped BaTiO3. Materials Characterization 15 (2): 1-6
[30]. Irzaman, Darvina Y, Fuad A, Arifin P, Budiman M, and Barmawi M (2003) Physical and pyroelectric properties of tantalum-oxide-doped lead zirconium titanate [$Pb_{0.9950}(Zr_{0.525}Ti_{0.465}Ta_{0.010})O_3$] thin films and their application for IR sensors. phys. stat. sol. (a) 199 (3) 416– 424
[31]. Irzaman, Pebriyanto Y, Apipah ER, Noor I, Alkadri A (2015) Characterization of Optical and Structural of Lanthanum Doped $LiTaO_3$ Thin Films. Integrated Ferroelectrics 167(1): 137-145
[32]. Irzaman, Putra IR, Aminullah, Syafutra H and Alatas H (2016) Development of ferroelectric solar cells of barium strontium titanate (BaxSr1-

xTiO3) for subtituting conventional battery in LAPAN-IPB Satellite (LISAT)," Procedia Environmental Sciences 33: 607-614

[33]. Irzaman, Sitompul H, Masitoh, Misbakhusshudur M and Mursyidah (2016) Optical and Structural Properties of Lanthanum Doped Lithium Niobate Thin Films. Ferroelectrics 502 (1): 9-18

[34]. Irzaman, Syafutra H, Rancasa E, Nuayi AW, Rahman TGN, Nuzulia NA, Supu I, Sugianto, Tumimomor F, Surianty, Muzikarno O, and Masrur (2013) The Effect of BaSr Ratio on Electrical and Optical Properties of $Ba_xSr_{(1-x)}TiO_3$ (x = 0.25; 0.35; 0.45; 0.55) Thin Film Semiconductor. Ferroelectrics 445 (1): 4-17

[35]. Izyumskaya, Alvov YA and Markac H (2013) High Oxide, Ferroelectrics, Ferromagnetics, and Multiferroics

[36]. Jesse S, Kim Y, Kumar A and Kalinin S (2012) Spectroscopic imaging in piezoresponse force microscopy: New opportunities for studying polarization dynamics in ferroelectrics and multiferroics. MRS Communication

[37]. Juraschek DM, Fechner M, Balatsky AV and Spaldin NA (2017) Dynamical multiferroicit, Physical Review Material 1: 1-9

[38]. Justin P, Michael S, Alois F and Eric S (2017) Powder selection for hydrothermally processed sol–gel composite barium strontium titanate capacitors. Phys. Status Solidi A 1-7

[39]. Kalinin Y, and Cao Y (2016) Phase-field modeling of chemical control of polarization stability and switching dynamics in ferroelectric thin films. Physical Review 11

[40]. Kang AH (2007) Ferroelectric Photonic Structures: Characterization and Device Demonstration

[41]. Khandelwa I, Adhikari R and Verma G (2015) Time Series Forecasting using Hybrid ARIMA and ANN Models based on DWT Decomposition. Procedia Computer Science 48: 173-179

[42]. Khan M, Nadeem MA and Idrissn H (2015) Ferroelectric Polarization effect on surface chemistry and photo-catalytic activity: Areview. Surface Science 31

[43]. Koutroumanidis T, Ioannou K, Garyfallos A. Predicting fuelwood pricesin Greece with the use of ARIMA models, artificial neural network and hybrid ARIMA-ANN model. Energy Policy 37: 3627-3634

[44]. Liang Z, Li S, Liu Z, Jiang Y, Li W, Wang T and Wang J (2015) High Responsivity of Pyroelectric Infrared Detector based on Ultra Thin LiTaO3

[45]. Lines M (1972) Nature of The Ferroelectric Paraelectric Phase Transition in Lithium Tantalate. Solid State Communication 10 (9): 793-796

[46]. Liu K, Chen Y and Zhang X (2017) An Application of the Seasonal Fractional ARIMA Model to the Semi conductor Manufacturing. IFAC Papers On Line 51 (1): 8097-8102

[47]. Li YH, Chen F, Xu GYGR and Wu W (2014) Ferroelectric, dielectric and leakage current properties of epitaxial (K,Na)NbO3-LiTaO3-CaZrO3 thin films. Springer Science Business Media New York 6.

[48]. Medeiros MC (2008) Modeling and forecasting short-term electricity load : Acomparison of methods with an application to Brazilian data. International Journal of Forecasting 24: 630-644

[49]. Mohan BR and Reddy GRM (2017) Resource Usage Prediction Based On Arima-Arch Model For Virtualized Server System. International Journal of GEOMATE 12 (33): 139-146

[50]. Morozova BLSP (2010) Monochromatic radiation source for calibration of the relative spectral sensitivy of earth observation instrumen. Measurement Technique 53

[51]. Naghi S and Mahmood B (2017) Synthesis and Characterization of Fe and Ni Co-Doped Ba0.6Sr0.4Tio3 Prepared by Sol-Gel Technique. Journal of Theoretical and Computational Science 4 (2): 1-6

[52]. Nelson BK (1998) Statistical Methodology : V. Time Series Analysis Using Autoregressive Integrated Moving Average (ARIMA) Models. Academic Emergency Medicine 5(7): 739-743

[53]. Nochai TNR (2006) ARIMA Model For Forecasting Oil Palm Price. Proceedings of the 2nd IMT-GT Regional Conference on Mathematics, Statistics and Applications

[54]. Oliveira PJ, Steffen JL and Cheung P (2017) Parameter Estimation of Seasonal ARIMA Models for Water Demand Forecasting using the Harmony Search Algorithm. Procedia Engineering 186: 177-185

[55]. Qin M, Li Z and Du Z (2017) Red tide time series forecasting by combining ARIMA. Knowledge-Based Systems 1-24

[56]. Reddy NI, Reddy VC, Cho MG and Shim J (2017) Morphological and chemical structure of silver-doped barium strontium titanate thin films fabricated via pulsed laser deposition. Mater. Res. Express 4: 1-13
[57]. Sharma R (2015) Nano particle technology ; formulating poorly water-soluble,compound : a review. IJPSR
[58]. Sharma S, Singh M, Mandala K and Shing NB (2015) Dielectric properties of low temperaturenano engineered Yttrium Copper Titanate ceramic 14
[59]. Shur VY, Mingaliev EA, Kosobokov MS, Makaev AV and Karpov VR (2017) Deposition of Droplets by Pyroelectric field created by Lithium Tantalate with Tailored Domain Structure. Ferroelectrics 508: 58-64
[60]. Sidorkin A, Nesterenko L and Darinskii ABM (2017) Switching processes of thin ferroelectric films, Accepted Manuscript 22
[61]. Soshnikov, Korobeinikov (2017) Mechanism For The Flash Under The Effect Of Monochromatic Radiation On Metal Surfaces. UDC
[62]. Sun E and Cao W (2014) Relaxor based Ferroelectric single crystal Growth, domain engineering, characterization and applications. Elsevier
[63]. Tavakoli M, Hajghassem H, Dousti M and Fathipour M (2013) Design and implementation of high data capacity RFID tag using eight-phase encoding. International Journal of Electronics
[64]. Trybula Z, Los S, Trybula M, Dec J and Miga S (2016) From Relaxor to Ferroelectric Behavior in $K_{1-x}Li_xTaO_3$. IEEE International Symposium on the Applications of Ferroelectrics, European Conference on Application of Polar Dielectrics, and Piezoelectric, 4 - 7
[65]. Varga T, Droubay TC, Kovarik L, Nandasiri MI, Shutthanandan V, Hu D, Kim B, Jeon S, Hong S, Li Y and Chambers SA (2017) Coupled Lattice Polarization and Ferro magnetism in Multiferroic NiTiO3 Thin Films. ACS Appl. Mater. Interfaces 1 (1): 1-40
[66]. Vogela U, Gemminga T and Eckerta SOJ (2016) Analysis of the thermal and temporal stability of Ta and Ti thin films on to SAW–substrate materials ($LiNbO_3$ and $LiTaO_3$) using ARXPS. Surface and Interface Analysis 5
[67]. Widowatia, Putro SP, Koshio S and Oktaferdiana V. Implementation of ARIMA Model toAsses Seasonal Variability Macrobenthic Assemblages. Aquatic Procedia 7: 277-284
[68]. Yanga M, Wanga J, Yana M, Goua J and Yadong ZW (2014) A Novel Sol-Gel Method of Preparation of the $LiTaO_3$ Thin Film and Its Property. An International Journal 9
[69]. Yogaraksa T, Hikam M, Irzaman (2004) Rietveld analysis of ferroelectric $PbZr_{0.525}Ti_{0.475}O_3$ thin films. Ceramics International 30: 1483–1485
[70]. Yoo BAJ (2012) Microstructure and Ferroelectric Properties of $(Na,K)(Nb,Sb)O_3$ Ceramics Substituted with $LiTaO_3$. Surface Science 8